https://rbgeomorfologia.org.br/
ISSN 2236-5664

Revista Brasileira de Geomorfologia

v. 26, nº 4 (2025)

http://dx.doi.org/10.20502/rbg.v26i4.2684

Research Article

Confined alluvial basins as evidence of recent tectonic conditioning of the drainage in the Northwestern Minas Gerais State, Brazil

Bacias aluvionares confinadas como indícios de condicionamento tectônico recente da drenagem no Noroeste de Minas Gerais

Mário Teixeira Rodrigues Bragança [1], **Luiz Fernando de Paula Barros** [2] and **Déborah de Oliveira** [3]

[1] Secretaria Municipal de Educação, Prefeitura Municipal de Betim, Betim/MG, Brasil. E-mail. mario.teixeira@alumni.usp.br
ORCID: https://orcid.org/0000-0003-2729-3619

[2] Departamento de Geografia, Instituto de Geociências, Universidade Federal de Minas Gerais, Belo Horizonte/MG, Brasil. E-mail. luizbarros@ufmg.br
ORCID: https://orcid.org/0000-0001-6122-4778

[3] Departamento de Geografia, Faculdade de Filosofia, Letras e Ciências Humanas; Departamento de Geologia Ambiental e Aplicada, Instituto de Geociências, Universidade de São Paulo, São Paulo/SP, Brasil. E-mail. debolive@usp.br
ORCID: https://orcid.org/0000-0002-3679-2893

Received: 04/03/2025; Accepted: 03/10/2025; Published: 10/11/2025

Abstract: This study investigated how alluvial sedimentation areas and compressed meanders in the confined basins of northwestern Minas Gerais State serve as evidence of recent tectonic restructuring. This was achieved by employing a morphotectonic approach that considers the sensitivity of river channels to small vertical and horizontal crustal variations. For this purpose, the drainage of the Paracatu and Urucuia River catchments at a scale of 1:100,000 was ordered, and images from the Google Earth Platform and numerical models of hypsometry, shaded relief, and slope were used to support visual inspections and the delimitation of confined basins. By applying morphometric and geomorphic indices, the shape and sedimentation patterns were assessed separately and comparatively in sections of fourth (or higher)-order channels that were considered anomalous. Moreover, a new methodological approach was proposed to quantitatively describe the channel dynamics within these basins. The indices showed correlations between confined basins, regional structural directions, and evidence of recent tectonic reactivation, as suggested by channel entrenchment and compressed meander sections. This study revealed that sediment accumulation occurred in specific sections. This accumulation is correlated with subsiding areas and the imposition of thresholds along channels, which are strongly linked to recent and low-intensity tectonic activity.

Keywords: Drainage anomaly; lithostructural control; Paracatu Structural High; confined basins; morphotectonics

Resumo: Esse trabalho investigou áreas de sedimentação aluvial e meandros comprimidos em bacias confinadas no Noroeste de Minas Gerais como indício de reestruturação tectônica recente, norteado pela abordagem morfotectônica e pela sensibilidade dos canais fluviais a pequenas variações verticais e horizontais da crosta. Para isso, a drenagem das bacias dos rios Paracatu e Urucuia, na escala de 1:100.000, foi ordenada; imagens da Plataforma Google Earth e modelos numéricos de hipsometria, relevo sombreado e declividade subsidiaram as inspeções visuais e a delimitação das bacias confinadas. Padrões de forma e de sedimentação em trechos de canais de quarta ordem ou superior, considerados anômalos, foram avaliados isolada e comparativamente, mediante aplicação de índices morfométricos e geomórficos; além disso, foi proposta uma nova abordagem metodológica para a descrição quantitativa da dinâmica dos canais no interior dessas bacias. Os índices mostraram correlação entre bacias confinadas, direções estruturais regionais e indícios de reativações tectônicas recentes, como sugerem o entrincheiramento de canais e os trechos de meandros comprimidos. O estudo revela que a acumulação sedimentar ocorre em trechos específicos, correlacionados tanto a áreas subsidentes quanto à imposição de soleiras ao longo dos canais, fatos que têm forte correlação com uma tectônica recente e de baixa intensidade.

Palavras-chave: Anomalia de drenagem; controle litoestrutural; Alto Estrutural do Paracatu; bacias confinadas; morfotectônica

1. Introduction

The high sensitivity of fluvial channels to abrupt topographic variations is a valuable indicator for exploratory studies of recent crustal movements (Rhea, 1989; Marple; Talwani, 1993; Pérez-Peña et al., 2009; Demoulin, 2011; Sougnez; Vanacker, 2011; Perucca et al., 2014; Manjoro, 2015). On cratonic platforms, where tectonic activity is significantly less pronounced than at plate margins, rivers respond to crustal deformations even when they are only weakly expressed in the topography (Burnett; Schumm, 1983). They rapidly adjust their course to substrate structures (Holbrook; Schumm, 1999) and zones of weakness (Cotton, 1951), or anomalously dissect these rocks and structures orthogonally (Twidale, 2004). Therefore, changes in riverbed lithology and adjustments in the channel course can be critical for drainage morphology and patterns (Lima, 2010), and for anomalies observed in river channels (Ramasamy et al., 2011).

When the channel deviates from the expected behaviour of the regional fluvial system, it is defined as anomalous, and its morphology becomes atypical (Howard, 1967; Pandey, 2001; Firmino; Souza Filho, 2017). These variations in river morphology, planform, and behaviour provide information on local structural patterns, active deformation, differential subsidence, drainage rearrangements, and changes in the hydrological regime (Howard, 1967). Therefore, drainage anomalies can serve as evidence of recent tectonic activity (Deffontaines; Chorowicz, 1991; Ramasamy et al., 2011; Souza; Rossetti, 2011). Anomalies in the sedimentation pattern, for example, may indicate that the drainage network is influenced by processes such as vertical block movements (Deffontaines and Chorowicz, 1991), shifts in sediment accumulation dynamics (Ramasamy et al., 2011), or the reorganisation of valley dissection (Bishop, 1985). Some of these processes result from the reactivation of ancient lithostructural features in passive margin and intraplate settings (Sordi et al., 2022); whereas others stem from responses to ongoing tectonic processes (Duvall et al., 2020).

In the contact zone between two Proterozoic Geotectonic Provinces, the São Francisco Craton and the Brasília Mobile Belt, a preliminary visual inspection of the Paracatu and Urucuia River catchments revealed entrenched channels and reaches with meanders confined by terraces with high scarps. In the Cotovelo Stream sub-catchment, the lower course is meandering, incised into a Holocene alluvial bed, and nested between the Pleistocene terraces located up to 30 m above the current channel (Bragança, 2022). The appraisal of these features points to the area's complex tectonic structure, indicating a subsiding basin (Bragança et al., 2002a). This basin appears to be controlled by SW-NE structural directions, which are correlated with the Meso-Cenozoic tectonic event (Campos; Dardenne, 1997).

Accordingly, this study characterise the spatial distribution of alluvial sedimentation areas and compressed meanders within confined alluvial basins in northwestern (NW) Minas Gerais. It also investigates their relevance as evidence of probable, low-intensity, and low-magnitude tectonic activity on a regional scale. The analysis is based on the principle that fluvial channels are sensitive to small vertical and horizontal crustal variations. These orographic-hydrographic relationships have become important references for morphotectonic investigations (Volkov et al., 1969), because anomalous channel behaviour can sometimes reflect recent crustal deformations of small magnitude and intensity (Guerasimov; Mescherikov, 1968).

2. Study Area

The study area covers the Paracatu and Urucuia River catchments, which are left-bank tributaries of the São Francisco River in NW Minas Gerais State (**Figure 1**). The Paracatu catchment spans ~45,000 km², and its highest headwaters lie above 1,120 m in the sources of the Preto River, north-west of the catchment; its mouth is at ~450 m, yielding a topographic amplitude of ~670 m. The Urucuia River catchment encompasses ~25,000 km²; its highest headwaters lie approximately 1,000 m from the sources of the Piratinga River, also in the north-west of the catchment, whereas its mouth lies at ~447 m with a topographic gradient of ~553 m.

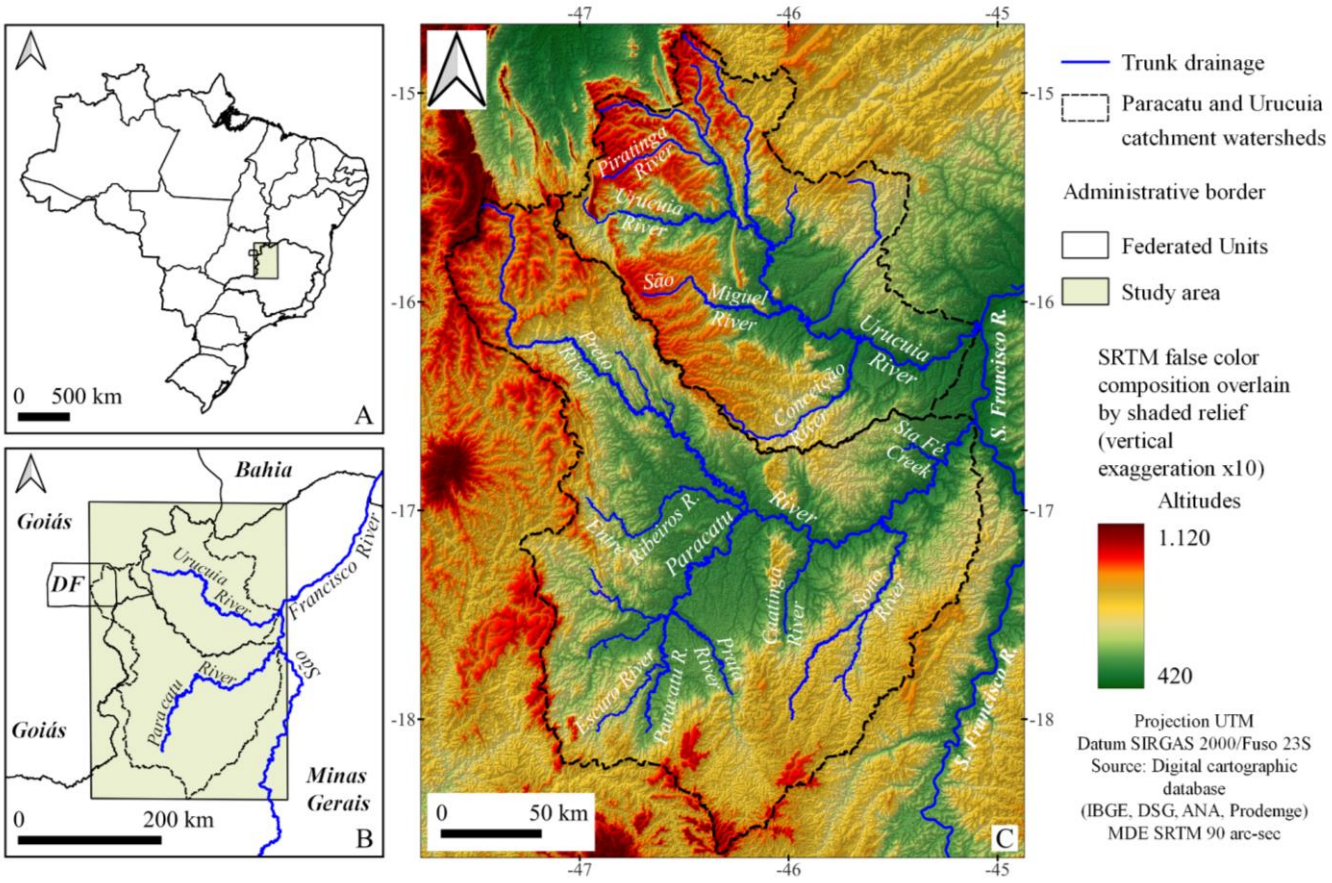

Figure 1. A) Location of the study area in relation to Brazil. B) Regional emplacement of the NW Minas Gerais State, highlighting the Paracatu and Urucuia River catchments and channels. C) Paracatu and Urucuia River catchments with main drainage and hypsometric model on the Shuttle Radar Topography Mission (SRTM) digital elevation model (DEM).

2.1. General aspects of the hydrographic network

In NW Minas Gerais, linearity, prominent parallelism, and anomalous changes in channel direction are prominent hydrographic features (Bragança et al., 2023). In general, this behaviour is directly related to both Precambrian and Meso-Cenozoic structural patterns (Bragança et al., 2022b). The Precambrian pattern comprises palaeo-strike-slip corridors and the São Domingos-Traçadal-Três Marias and Unaí-João Pinheiro-Galena fault zones, with dominant NNW-SSE structural trends; approximately 40 km eastward of, and parallel to, the structural contact between the São Francisco craton and the Brasília fold belt, lies a NNW-SSE shear zone, a Precambrian tectonic feature (Campos; Dardenne, 1997a; CPRM, 2003a; 2003b), correlated with the Paraopeba Tectonics (Schobbenhaus et al., 1984). Superimposed upon the Precambrian pattern are intersections with the Meso-Cenozoic structural pattern defined by near-surface faulting with a dominant SW-NE orientation (Campos; Dardenne, 1997). Their intersection generates abrupt channel direction changes, forming elbows or anomalous bends (Bragança et al., 2022b; 2023a). Additionally, areas of channel entrenchment occur within the aforementioned fault zones and in sedimentary domains, evidencing disequilibrium at the regional base level and a tendency for incision along the main channels (Bragança et al., 2022c).

2.2. Regional geology

The study area corresponds to an Upper Proterozoic–Lower Palaeozoic (Brasiliano Tectonic Cycle), tectonically structured, sub-meridian province, encompassing the contact between the Brasília Fold Belt and the São Francisco Craton, as well as the deformed cratonic coverage of the foreland basin in its western domain (**Figure 2**). Lithologies represented include the Bambuí Group (Upper Proterozoic), Santa Fé Group (Upper Paleozoic), Areado Group (Middle Cretaceous), Urucuia and Mata da Corda Groups (Upper Cretaceous), and Neo-Cenozoic

alluvial-colluvial covers of a predominantly sandy and sandy-clayey nature, occasionally lateritic (Moreira; Camelier, 1977; Campos; Dardenne, 1997b). The Bambuí Group consists predominantly of pelite-carbonated sequences, arkosic sandstones and siltstones, epi- and syn-tectonic in origin (Campos; Dardenne, 1997b). The Santa Fé Group is glaciogenic and comprises tillite and diamictite sequences with varves and dropstones in shales (Campos; Dardenne, 1994).

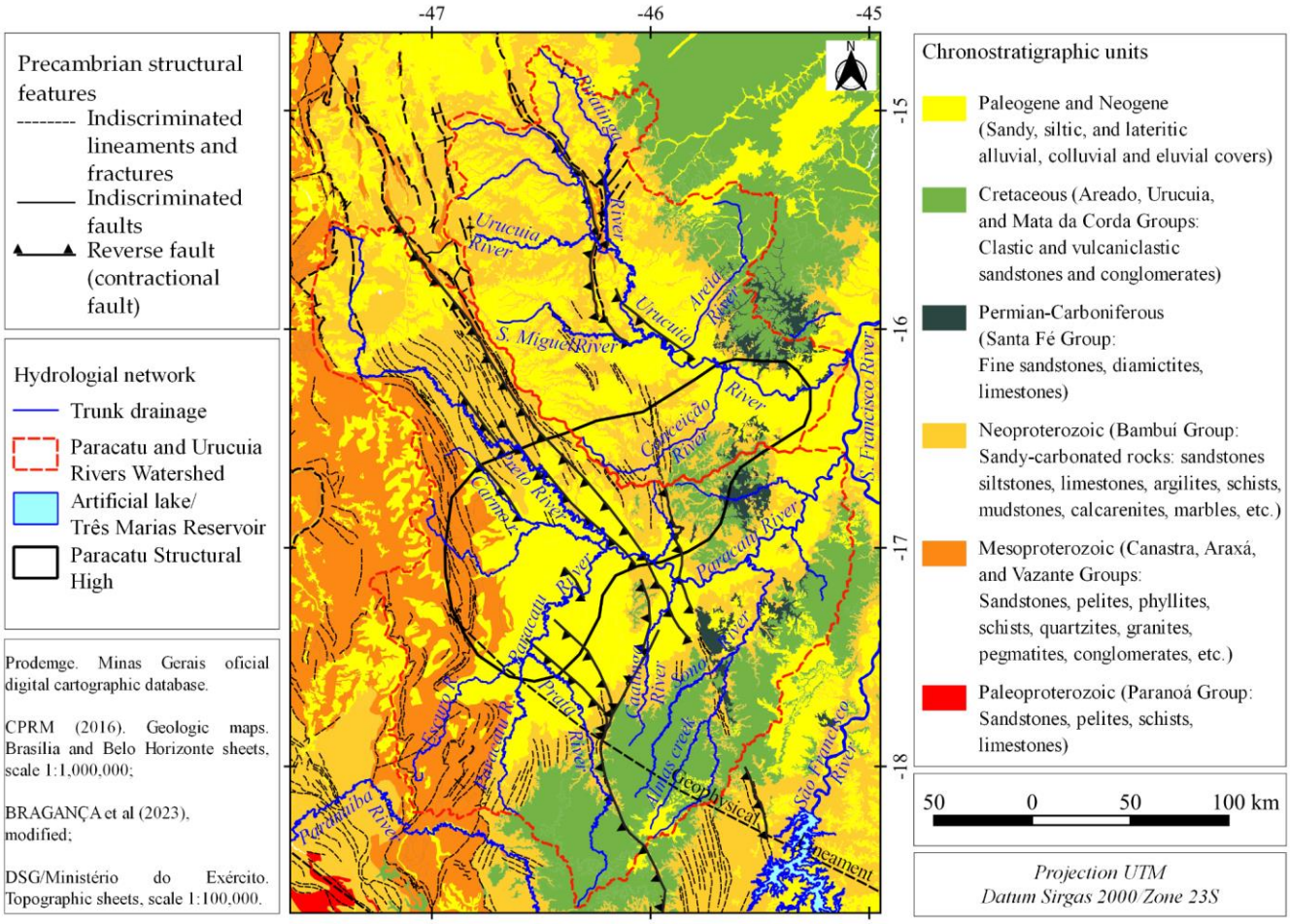

Figure 2. Lithostructural map of the NW Minas Gerais State.

Mesozoic Formations occur at the highest elevations and are lithologically diverse. Basal conglomerates containing ventifacts and aeolian and fluvial sandstones mark the lower boundary of the Mid-Cretaceous. The upper sections are shales, siltstones, and fine-grained sandstones of lacustrine and shallow-marine settings, along with channel, floodplain, and fluvial-deltaic facies (Barcelos; Suguio, 1980; Kattah, 1991; Campos and Dardenne, 1994; Campos; Dardenne, 1997a; Sgarbi, 2000). Medium-grained sandstones of desert systems with fluvial, lacustrine, and aeolian facies (Urucuia Group) assigned to the Upper Cretaceous (Campos and Dardenne, 1994, 1997b), overlie the previous units; they crop out as cappings and cornices and are locally silicified (Sgarbi, 2000). The Urucuia sandstones intertongue laterally with volcaniclastic sandstones derived from mafic and ultramafic tuffs and lavas of the Mata da Corda Group (Fragoso et al., 2011), dated to ~80 Ma (Campos and Dardenne, 1994, 1997b).

Neo-Cenozoic alluvial, colluvial, and eluvial covers, formally termed the Chapadão Formation (Moreira; Camelier, 1977), comprise unconsolidated detrital sediments, predominantly sandy, but also sandy-clayey, silty, and clayey-silty, with or without pebbles and boulders, derived from remobilisation and reworking of older covers (Campos Dardenne, 1997b); finer materials infill numerous lakes and dolines, mainly within the Paracatu catchment (Minas Gerais, 1983; CPRM, 2003a, b; Almeida et al., 2011).

Within this varied and complex lithostratigraphic framework lies the Paracatu Structural High, a positive Precambrian tectonic feature described from elevation differences at the contact between the metasedimentary rocks of the Bambuí Group and the Phanerozoic cover, and from variations in the sedimentary-succession

thickness (Campos; Dardenne, 1997a). It is 'a tectonic feature resulting from basement uplift attributed to flexural re-equilibrium mechanisms of the lithosphere in response to lateral overloading associated with Brasiliano tectonics' (Campos; Dardenne, 1997a). Superposed on this is a NNW-SSE shear zone of mid- to late-Proterozoic age derived from Paraopeba tectonism, which deformed the PreCambrian cratonic cover (Schobbenhaus et al., 1984, 1985; CPRM, 2003a, b). This zone marks the contact between two distinct geotectonic compartments: to the west, the external (eastern) domain of the Brasília Fold Belt, with vergence towards the craton and intensely deformed rocks; to the east, the Bambuí Sequence, in which stratigraphic units remain practically undeformed away from the tectonic contact (Alkmim et al. 1993; Alkmim; Martins-Neto, 2001). The contact zone displays a dense network of crustal fractures and lineaments preferentially oriented from NNW-SSE to NW-SE, which is attributable to transpressional tectonics (CPRM, 2003a; 2003b).

This fracture network was complicated by six tectonic stages that recorded the structural evolution of the Sanfranciscan cratonic cover during the Palaeozoic and Meso-Cenozoic (Campos; Dardenne, 1997a), as reflected by the main regional structural features. These continuous tectonics resulted from Gondwana fragmentation and the drift of the South American plate, whose effects are perceived in the reactivation of Brasiliano structures, development of rift-related processes, flexural subsidence, Mata da Corda magmatism, and neotectonic reactivation (Hasui, 1990; Hasui; Haralyi, 1991; Saadi, 1991; Campos; Dardenne, 1997a).

The study area records a few significant volumes of Quaternary sediment bodies, largely restricted to Upper Pleistocene and Holocene alluvial deposits. Two well-defined alluvial levels were identified in the landscape.

The older, higher level occurs above ~530 m, with surfaces positioned 30–50 m above the present channels, and ages between 76,500 and 12,100 years. This unit has a flat top, but its boundary with the floodplain is often a gently inclined ramp towards the modern channel. It comprises unconsolidated sand sediments, beige to yellowish, produced by reworking of alder covers and redistributed on terraces along the Paracatu and Urucuia rivers and their main tributaries; when remobilised by recent processes, these materials may also spread across the floodplain. Locally, these terraces contain lenticular beds of abundant rounded pebbles derived from the Três Marias Formation sandstone (COMIG; CPRM, 2003a; 2003b; Bragança et al., 2022).

The younger, lower level occurs ~500 m upward, with surfaces positioned 4–20 m above modern channels. Sandy facies (coarse and medium sand) are present, with ages between ~4,300 and ~1,100 years (Bragança et al., 2022). Mapped as 'alluvium', this unit comprises unconsolidated sediments of sandy, sandy-clayey, and clayey-silty nature, beige to yellowish, with banks/terraces of coarse gravels and possible cobles and boulders of quartz, quartzite, sandstone, mudstone, siltstone, limestone, and chert. They result from the reworking of alder covers and are redistributed on terraces and floodplains of the Paracatu and Urucuia Rivers, generally above 500 m (COMIG; CPRM, 2003a; 2003b), although they are also observed at lower elevations downstream of the Cotovelo River mouth.

2.3 Regional geomorphology

The NW Minas Gerais State landscape comprises four geomorphological regions (Minas Gerais, 1981, 1983; Nunes et al., 1995): the São Francisco Plateaus (associated with Phanerozoic sedimentary covers), the São Francisco Plain and São Francisco Depression (associated with Quaternary sedimentary deposits), and the Unaí Ridges (associated with the Neoproterozoic Brasília Fold Belt). **Figure 3** shows the principal geomorphological units overlain by regional-scale structural features associated with the four aforementioned geomorphological regions. Thus, the map attained the third taxonomic level of the methodological framework (Nunes et al., 1995).

The São Francisco Plateaux contains the highest regional topographic compartments (700–950 m), carved predominantly into Neoproterozoic arkosic sandstones of the Três Marias Formation (Bambuí Group) and Cretaceous siliciclastic sandstones (Areado and Urucuia Groups), and are frequently mantled by thick Cenozoic sandy and sandy-clayey packages (Chapadão Formation). The morphology ranges from flat-topped (chapadas) and gently undulating surfaces to elongated valleys incised by low-order streams entrenched in the bedrock, which produce rapids and riffles (Moreira; Camelier, 1977; CETEC, 1981, 1983; Campos; Dardenne, 1997). On plateau margins, spectacular waterfalls mark topographic breaks; small, isolated residual tops can reach ~1,100 m (Bragança, 2012). The plateau dips east-south-southeast towards the São Francisco River drainage (CETEC, 1981).

The Unaí Ridges comprises a ridge-and-valley terrain controlled by elongated folds trending NNW, associated with WSW-dipping reverse faults that affect the Bambuí Group and older arenaceous strata (Coelho et

al., 2008; Reis et al., 2012). A typical WSW-ENE topographic profile records valley floors at~550–590 m and ridge crests at ~ 730–790 m.

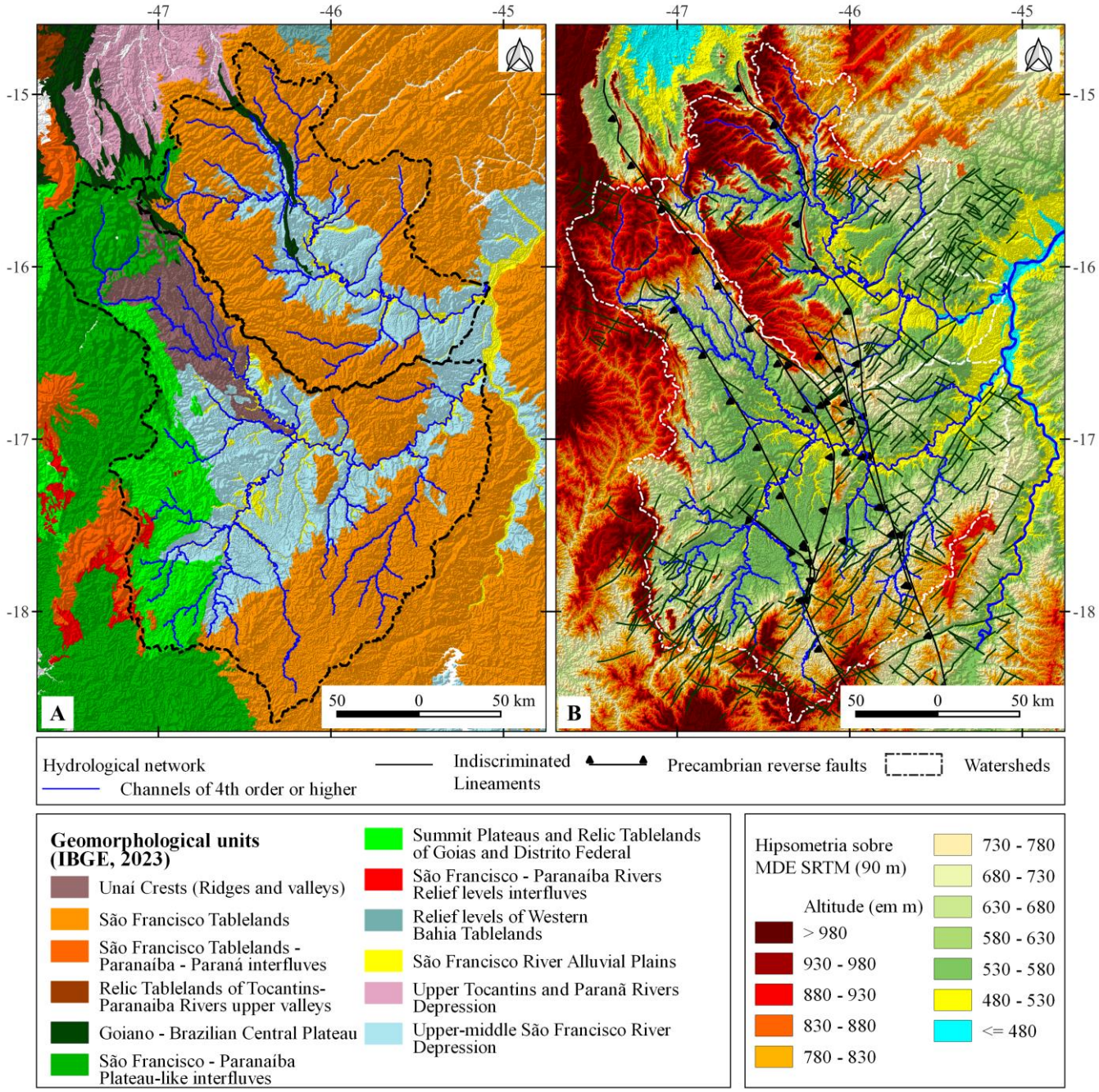

Figure 3. Geomorphological aspects of NW Minas Gerais State. A) Geomorphological units (modified from IBGE, 2023). B) Hypsometry, main structural features and crustal lineaments (NNW-SSE and SW-NE), on a regional scale. Reverse faults modified from Minas Gerais (1981); lineaments modified from Bragança et al. (2023). Drainage from the GeoMinas Project (2017). Hypsometry processed on the SRTM DEM, with 90 m-spatial resolution.

Plains and depressions exhibit exceptionally flat, regular morphologies following the São Francisco River and its main tributaries, with elevations ranging from ~480 to ~530 m, which coincide with stacks of recent alluvial sediments of Pleistocene to Holocene ages (CPRM; COMIG, 2003a; 2003b; Bragança et al., 2022b). In the western sector of the Paracatu River catchment, west of the Serra da Maravilha, the morphology coincides with the carbonate rocks of the Serra da Saudade and Lagoa do Jacaré Formations, locally generating karst depressions with spongillite deposits (Almeida et al., 2011). Plains and depressions are typically bounded by (i) low rounded hills, ramps, and low plateaus marking the transition to elevations above ~600 m or (ii) vertically oriented scarps,

possibly fault scarps, such as along the western margin of the Serra da Maravilha and the entire southwestern margin of the Serra Geral do Rio Preto.

Geomorphologically, terraces and floodplains were significant throughout the study area owing to their extent and the imposing terrace scarps, particularly along the small tributaries of the Paracatu and Urucuia Rivers.

Figure 4 shows representative landform units of NW Minas Gerais State, highlighting the magnitude and exuberance of these features, considering the regional-scale approach of this research.

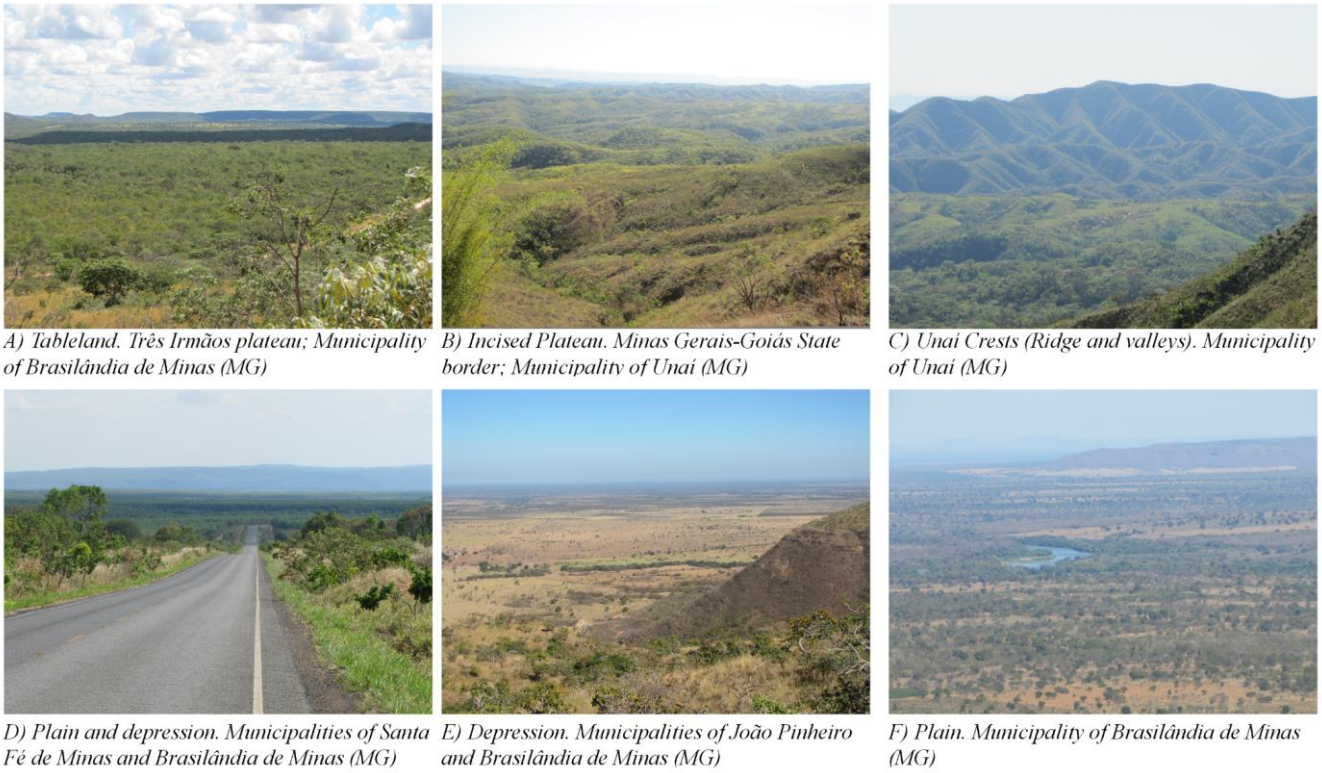

Figure 4. Landform units of NW Minas Gerais State. Photographs: collection of the first author.

3. Materials and Methods

To delimit landform units in NW Minas Gerais State, relevant structural/tectonic features were recorded, and a regional hypsometric model was processed using 13 primary C-band Interferometric Synthetic Aperture Radar–SRTM scenes (LP-DAAC, 2018) at a 90 m spatial resolution (unresampled).

Next, regional hypsometry, shaded relief, and slope models were processed from 44 scenes of the Phased Array L-band Synthetic Aperture Radar (Palsar) digital elevation model (DEM) with a 12.5 m spatial resolution and high-resolution terrain radiometric correction (ASF-DAAC, 2018). Processing was conducted in QGIS (QGIS Development Team, 2023) over an envelope polygon covering the Paracatu and Urucuia River catchments, and the outputs underpinned the delimitation of sedimentation basins at a scale compatible with the objectives of the study.

Within the regional frame, hypsometry captured a total relief of ~673 m, distributed into classes with 5 m intervals between 443 and 700 m elevation; above 700 m, 25 m intervals were used. These intervals reflect two well-marked geomorphic patterns: (a) below 700 m, hillslopes are heavily dissected by channels incised into the bedrock and strongly controlled by a dense fracture network as well as by thick alluvial packages (Bragança, 2022; Bragança et al., 2022b), requiring greater hypsometry details; and (b) above 700 m, the regularly flat morphology offers little information for the present regional-scale approach.

In QGIS, the resulting hypsometric model was multiplied by shaded-relief maps with at least four illumination azimuths (45º, 135º, 225º, and 315º), adapting a map-algebra methodology that combines DEM-derived images (Chuvieco, 1996; Drachal; Debowska, 2014). The optimal solar-elevation angles were determined (25º, 28º, 35º, 45º). Vertical exaggeration was set to x10. These products also supported the extraction of topographic profiles.

3.1 Systematisation of the drainage-network database

The attribute table for the 1:100,000 vector drainage network (Prodemge, n.d.) was manually updated and ordered following Strahler (1957), and this topographic map scale was adopted for the study. The hydrography was then overlain on terrain models and Google Earth satellite imagery for visual inspection; overlay was performed directly using the imagery available via the homepage after importing into the QGIS project. Visual analysis of the DEM-derived thematic products enabled evaluation and mapping of the drainage features of interest.

3.2 Identification of anomalies in drainage channels

Drainage anomalies are defined as 'local deviations from drainage and flow patterns that elsewhere accord with known regional geology and topography' (Howard, 1967). Anomalies are considered to be compressed meanders associated with alluvial sedimentation within confined accumulation basins (Zernitz, 1932; Howard, 1967; Ramasamy et al., 2011). Conceptualised, confined alluvial basins are sediment-accumulation areas circumscribed between higher terrains and widened or narrow and elongated, in which channel velocity is reduced by the presence of bedrock sills or by vertically mobile blocks (subsiding or uplifted), and sediment deposition promotes the development of meanders and increases meander length. This approach recognises that straight and strongly confined channels adjusted to lithostructural zones of weakness predominate regionally (Bragança et al., 2023a).

These procedures also underpinned the spatial selection of field-check sites. At each site, the bedding dip and dip direction (primary structures), azimuth, and dip/dip direction of fractures and folds (secondary structures) were recorded. Panoramic photographs provided contextualisation of the anomalies and supported the interpretation.

3.3 Mapping alluvial sedimentation and compressed meanders in confined alluvial basins

Mapping of confined alluvial basins was based on hypsometric models derived from the Palsar DEM and on high-resolution Google Earth imagery, imported and manipulated in QGIS. The Palsar DEM was supplied as a GeoTIFFs at UTM/ WGS84. Google Earth imagery is compatible with the same data. The QuickMapServices plugin was used for image insertion and overlay operations.

Integral overlay and manipulation of both products were performed using their native georeferencing. QGIS automatically handled projection and coordinate-system transformations, enabling direct overlay, and the following features of interest were digitised: basin perimeters, active channel courses inside basins, and terrace scarps. This produced a vector database (shapefiles) whose positional accuracy proved compatible with a 1:10,000 scale, as assessed by Lopes (2009), mainly because of the prevalence of low-relief terrain in the area.

Basin perimeters were drawn to encompass recent sedimentation areas, preserving the topographic marks of channel dynamics (e.g. terrace scarps and hydromorphic limits). These products were overlaid on high-resolution imagery and, when necessary, multiplied to enhance feature visibility. The confined alluvial basins were identified by visual inspection of satellite images and channel traces. The basin perimeters were digitised from the terrace edges that confine the modern floodplain.

3.4 Geometric parameters of confined alluvial basins

To investigate sedimentation dynamics and channel migration within confined alluvial basins, a methodological proposal (**Figure 5**) was developed. The basin perimeter (P) and area (A) of each confined floodplain were measured using Google Earth. The main channel within the delimited area was traced to obtain the channel length within the meandering reach (Lc) and its straight-line length (L). Using MapInfo Professional, the central axis (E) was drawn equidistant from the basin margins, and its length was measured.

For each basin, we collected multiple width (W) transects using the Google Earth ruler, drawing perpendiculars to the channel and to basin width designed to intercept all meanders; the sample of n measurements provided a mean width ($\bar{x}W$) and standard deviation (σW). Next, measured distances between the convex limbs of abandoned meanders (geomorphic traces and oxbow lakes) and the current position of the main channel (D), yielding a sample of n measurements from which the mean active-meander-belt width ($\bar{x}D$) and its standard deviation (σD) were obtained.

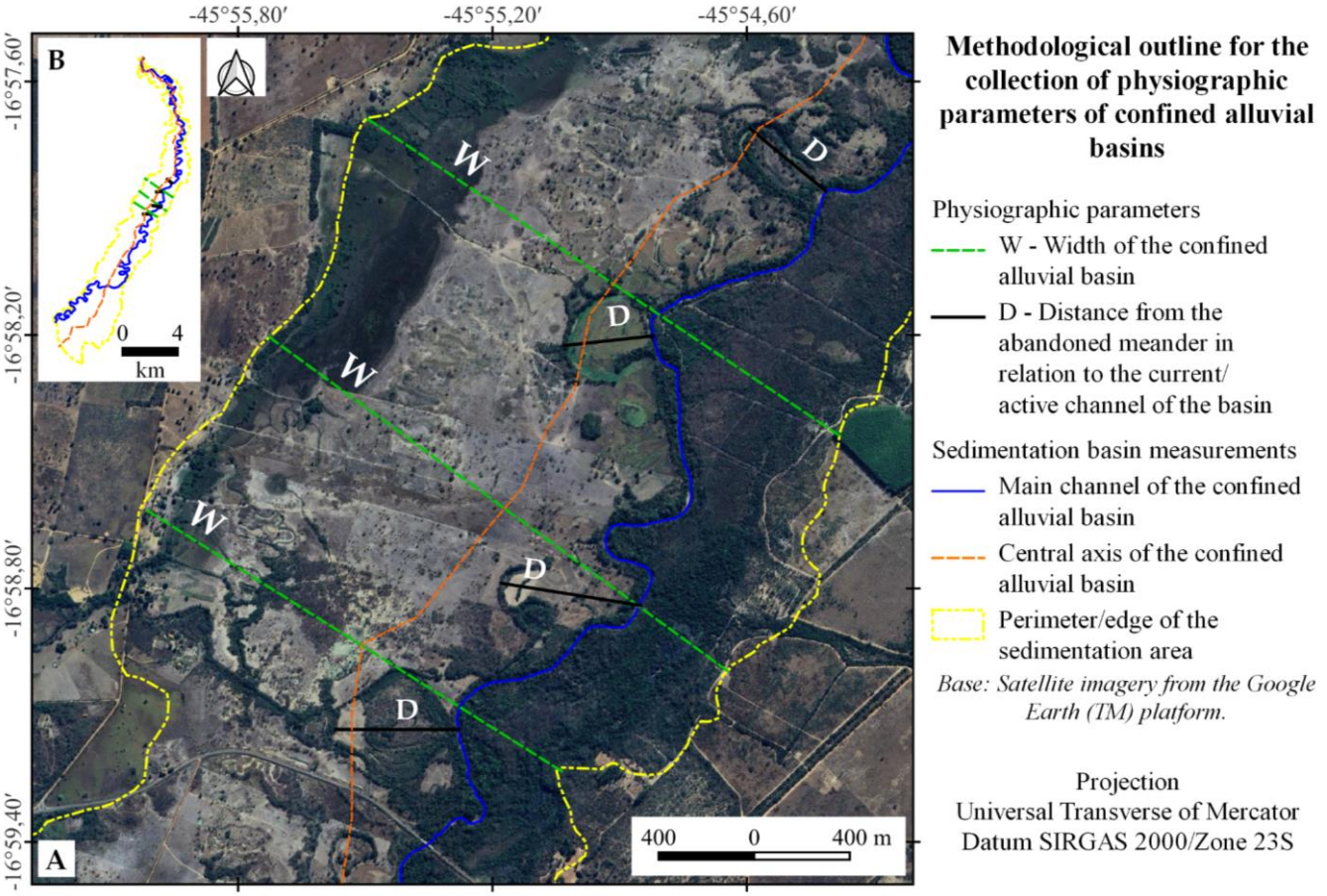

Figure 5. Details of the procedures for obtaining the geometric parameters used to assess the confined alluvial basins. A) Routines for measuring the width of the confined alluvial plains (W) and the distance of the abandoned meanders in relation to the current channel of the plain (D). B) Demarcation of the central axis of the confined alluvial plain.

3.5 Morphometric and geomorphic analysis of confined alluvial basins

Confined alluvial basins were analysed using established morphometric and geomorphic indices: Sinuosity Index (Si; Villela; Mattos, 1975), applied to the river reach within the basin to assess degree of meandering; Compactness Coefficient, (Kc; Villela; Mattos, 1975), applied to basin shape to measure the regularity relative to a perfect circle; the Basin Asymmetry Factor, (Af; Hare; Gardner, 1985) and Transverse Topographic Symmetry Factor (TTSF; Cox, 1994), to assess possible asymmetries in the development of sedimentation areas. Although the Kc, Af, and TTSF were originally proposed for drainage basin analysis, they were applied to confined alluvial basins to provide a comparative description and systematic assessment of their morphology.

For Af (Hare; Gardner, 1985), the classes were adjusted according to Pérez-Peña et al. (2010) as follows:

Class 1: Af < 5 (class 1, symmetrical basins);
Class 2: Af = 5-10 (class 2, gently asymmetrical basins);
Class 3: Af = 10-15 (class 3, moderately asymmetrical basins);
Class 4: Af > 15 (class 4, strongly asymmetrical basins).

For the TTSF (Cox, 1994), the values were grouped into the following descriptive classes (Salvany, 2004):

Class 1: TTSF < 0.2 (low tilt);
Class 2: 0.2 ≤ TTSF < 0.4 (moderate tilt);
Class 3: TTSF ≥ 0.4 (pronounced tilt).

All indices were computed and confined sedimentation basins were mapped using QGIS from available databases (Prodemge, n.d.).

4. Results and discussion

The confined alluvial basins identified in NW Minas Gerais State correspond to channel reaches where rivers flow through thick alluvial packages. These reaches are bounded by near-vertical terrace scarps that can exceed 30 m in height. Inside these areas, the channels follow meandering courses with pronounced sinuosity. These basins approach the concept of wetlands (Gomes; Magalhães Jr, 2020) in definition and environmental functions and play crucial hydrogeomorphological roles in the preservation of fluvial systems, contributing to water quality protection, flood-regime moderation, aquifer recharge, and perennial surface water. These properties are apparent given that NW Minas Gerais State lies within a typical tropical climate domain marked by regular water stress. Eleven confined alluvial basins were identified and mapped: five and six in the Paracatu and Urucuia River catchments, respectively (**Figure 6**).

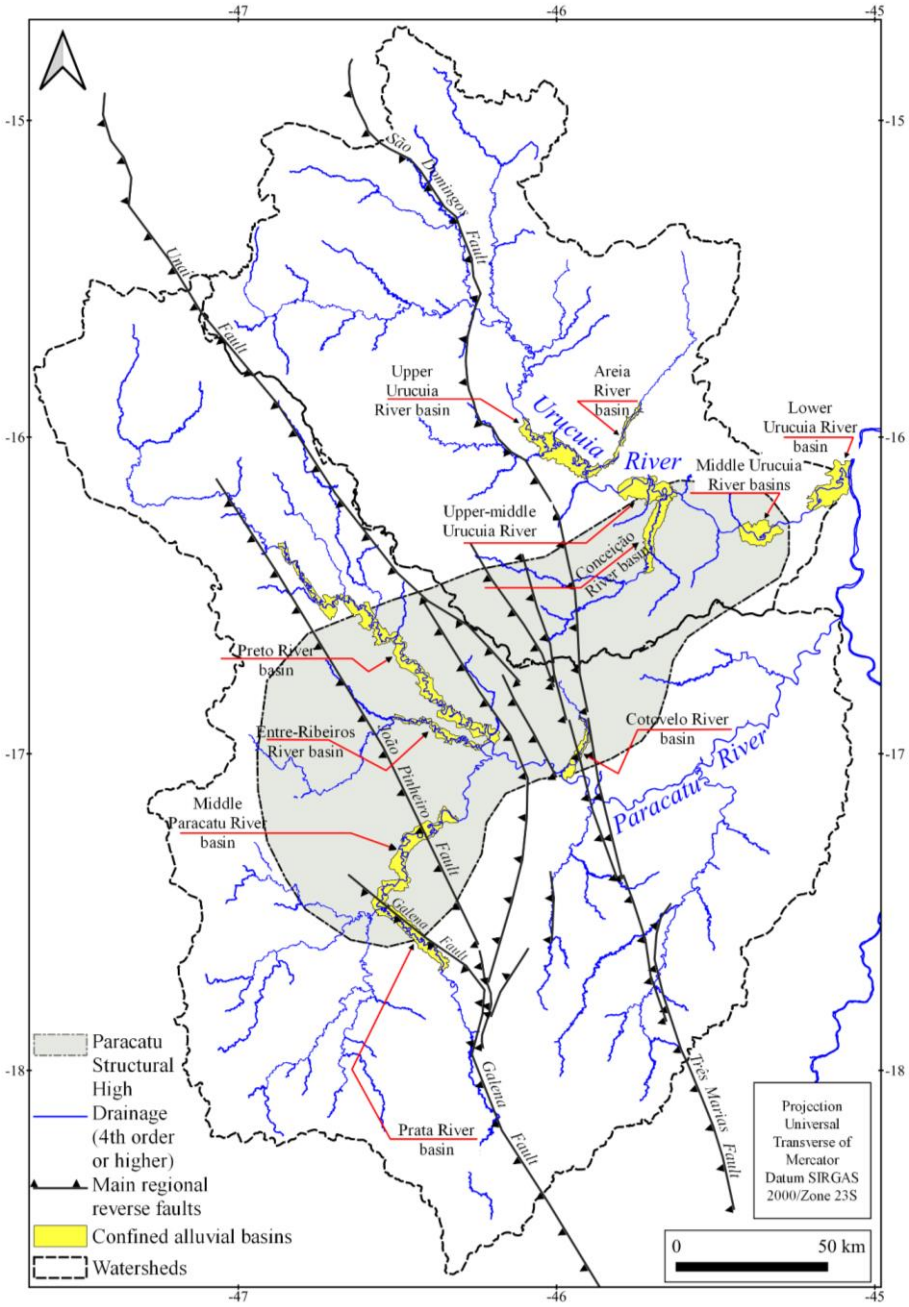

Figure 6. Confined alluvial basin and compressed meanders in the Paracatu and Urucuia River catchments. Indication of the main reverse faults (Modified from Schobbenhaus et al., 1985; Campos; Dardenne, 1997b), indiscriminate lineaments (Modified from Bragança et al., 2023) and the Paracatu Structural High (modified from Campos; Dardenne, 1997b).

These confined basins were generally elongated. Their genesis is associated with an upstream reach comprising an approximately straight channel incised into the bedrock, where the flow velocity decreases and bedload deposition becomes predominant, producing a broad sedimentary plain within which the channel adopts a meandering planform. Sills can be observed in the Cotovelo River channel between the confluences of the Alegre and Cana-Brava streams (**Figure 7**). After traversing the confined sedimentation basins, the channels resume a straight reach.

For the Preto River specifically, the channel meanders within the Unaí Ridges landform unit; dissection exposes the rugged topography of ridges and incised valleys developed in carbonate rocks of the Serra da Saudade and Lagoa do Jacaré Formations and correlates with numerous structural weakness zones in a substrate intensely fractured and sheared along the tectonic contact between craton and fold belt (Alkmim; Martins-Neto, 2001; CPRM, 2003a; 2003b; Reis; Alkmim, 2015; Reis et al., 2017).

The confined alluvial basins mapped in the Paracatu River catchment are slightly more elongated than those mapped in the Urucuia River catchment. In the Paracatu River catchment, they are located in the upstream sector (west of Serra da Maravilha), except in the lower Cotovelo River valley. Only one basin is associated with the Paracatu River trunk stream, and the remainder occurs along tributaries. In the Urucuia River catchment, confined alluvial basins are smaller and more rounded; they are distributed along the trunk stream, with only two associated tributaries (the Conceição and Areia Rivers).

This pattern reflects stronger differential control of the Urucuia River by the São Domingos fault zone, along which structural barriers perpendicular to the fault are evident. Another contributing factor is that the Paracatu River catchment is more dissected and wider to the west, whereas the Urucuia River catchment is more elongated and dips E-SE towards the São Francisco River, favouring the incision of the main drainage, channel orientation, and more aggressive dissection towards the base level.

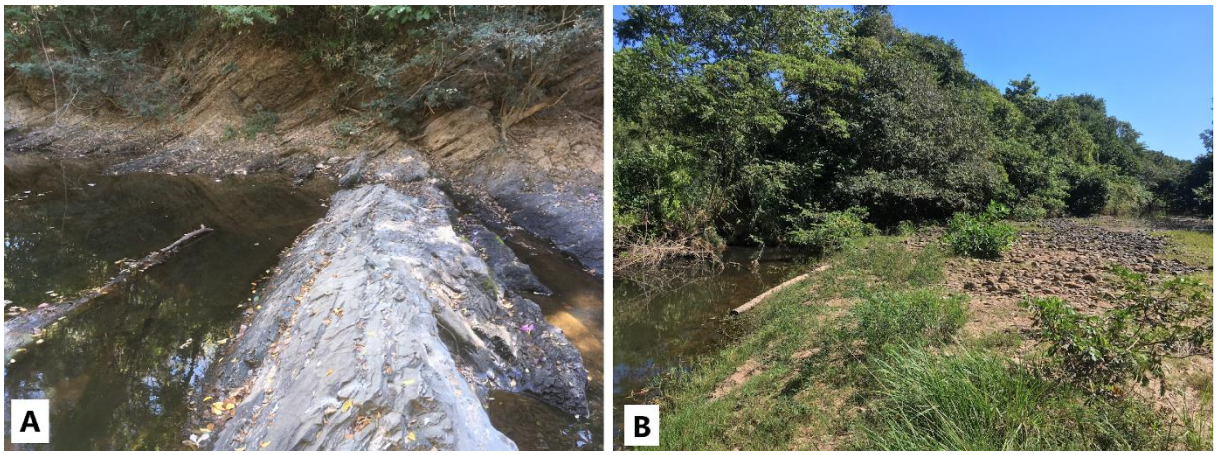

Figure 7. Examples of sills along the Cotovelo River channel. A) Outcrop of limestone from the Serra da Saudade formation. B) Natural obstacle resulting from the paving of the riverbed by the accumulation of pebbles. Photographs: collection of the first author.

4.1 Assessment of confined alluvial basins using morphometric and geomorphic indices

Quantitative treatment of variables and the application of morphometric and geomorphic indices enabled individual quantitative assessments of the basins and subsequent comparative analyses. Below, **Tables 1–4** summarise the principal patterns derived from Kc, Si, Af, and TTSF.

Table 1. Physiographic and geometric parameters of confined alluvial basins, mapped in the Paracatu River catchment.

Paracatu catchment basins	Lc	L	A	n (W)	$\bar{X}$ (W) ± σ (W)	n (D)	$\bar{X}$ (D) ± σ (D)	E	P
Prata River	67,2	29,9	108,8	14	3.257,2 ± 778,5	24	1.296,4 ± 705,9	31.341	90,3
Entre-Ribeiros River	76,5	31,8	67,8	33	1.875,6 ± 848,9	52	598,7 ± 373,2	33.554	97,4
Preto River	239,8	99,0	382,9	33	2.778,9 ± 1.315,2	33	988,6 ± 638,6	114.264	321,0
Paracatu River	40,0	103,6	199,1	19	4.352,9 ± 1.564,5	26	1.635,5 ± 931,2	50.593	129,0
Cotovelo River	45,6	20,9	52,7	19	2.078,5 ± 998,8	31	394,7 ± 187,7	25.487	68,7

Lc: Length of the channel in the meandering area (in km); L: Linear length of the compressed meander segment/sedimentation area (in km); A: area of the polygon containing the active meander strip (km²); W: width of the confined sedimentation plain (in m); n (W): number of samples used to calculate the mean value of W (in m); $\bar{X}$ (W): mean width of the active meander strip (in m); σ: standard deviation of the sample (in m); D: linear distance between the concave section of the abandoned meanders and the active channel of the confined floodplain (in m); n (D): number of samples used to calculate the mean value of D (in m); $\bar{X}$(D): average distance between the abandoned meanders and the active channel of the confined floodplain; E: length of the central axis of the basin (in m); P: basin perimeter (in km).

Table 2. Physiographic and geometric parameters of confined alluvial basins, mapped in the UIrucuia River catchment.

Urucuia catchment basins	Lc	L	A	n (W)	$\bar{X}$ (W) ± σ (W)	n (D)	$\bar{X}$ (D) ± σ (D)	E	P
Urucuia River upper valley	85,45	30,12	173,85	19	4.564,1 ± 2.027,4	38	2.163,0 ± 1.628,1	31.785	108,0
Urucuia River upper-middle valley	37,49	19,81	125,34	19	6.575,8 ± 1.908,2	35	2.163,5 ± 1.614,7	21.013	67,7
Urucuia River middle valley	23,66	12,2	87,13	12	6.250,8 ± 2.069,2	16	2.216,1 ± 1.226,4	15.385	49,4
Urucuia River lower valley	38,89	17,27	126,43	19	6.411,6 ± 2.434,6	17	1.332,1 ± 956,4	17.255	74,2
Areia River	55,64	25,98	34,99	27	1.300,9 ± 376,0	49	371,7 ± 293,0	27.347	78,7
Conceição River	54,66	24,04	100,6	20	3.221,0 ± 1.045,1	60	850,0 ± 477,3	29.268	79,5

Legend as per Table 1.

Table 3. Quantitative description of confined alluvial basins, mapped in the Paracatu River catchment.

Confined alluvial basins	W ± σ (m)	A (km²)	D ± σ (m)
Prata River	3.257,2 ± 778,5	108,78	1.296,4 ± 705,9
Entre-Ribeiros River	1.875,6 ± 848,9	67,82	598,7 ± 373,2
Preto River	2.778,9 ± 1.315,2	382,89	988,6 ± 638,6
Paracatu River	4.352,9 ± 1.564,5	199,09	1.635,5 ± 931,2
Cotovelo River	2.078,5 ± 998,8	52,72	394,7 ± 187,7

W ± σ (m): Average width ± the standard deviation of this average width, in meters; A: Basin area, in km²; D: average distance of the abandoned meander belt in relation to the active channel ± the standard deviation of this average distance, in meters.

Table 4. Quantitative description of confined alluvial basins, mapped in the Urucuia River catchment.

Confined alluvial basins	W ± σ (m)	A (km²)	D ± σ (m)
Urucuia River upper valley	4.564,1 ± 2.027,4	173,85	2.163,0 ± 1.628,1
Urucuia River upper-middle valley	6.575,8 ± 1.908,2	125,34	2.163,5 ± 1.614,7
Urucuia River middle valley	6.250,8 ± 2.069,2	87,13	2.216,1 ± 1.226,4
Urucuia River lower valley	6.411,6 ± 2.434,6	126,43	1.332,1 ± 956,4
Areia River	1.300,9 ± 376,0	34,99	371,7 ± 293,0
Conceição River	3.221,0 ± 1.045,1	100,6	850,0 ± 477,3

Legend as per Table 1.

Figures 8 and 9 present the results for *Si, Kc, Af, TTSF, Standard Deviation of the TTSF values,* and *Percentages of areas on the right and left banks and histogram*, indicating the main directions of migration of the channels of each of the confined alluvial basins of the Paracatu and Urucuia Rivers, respectively.

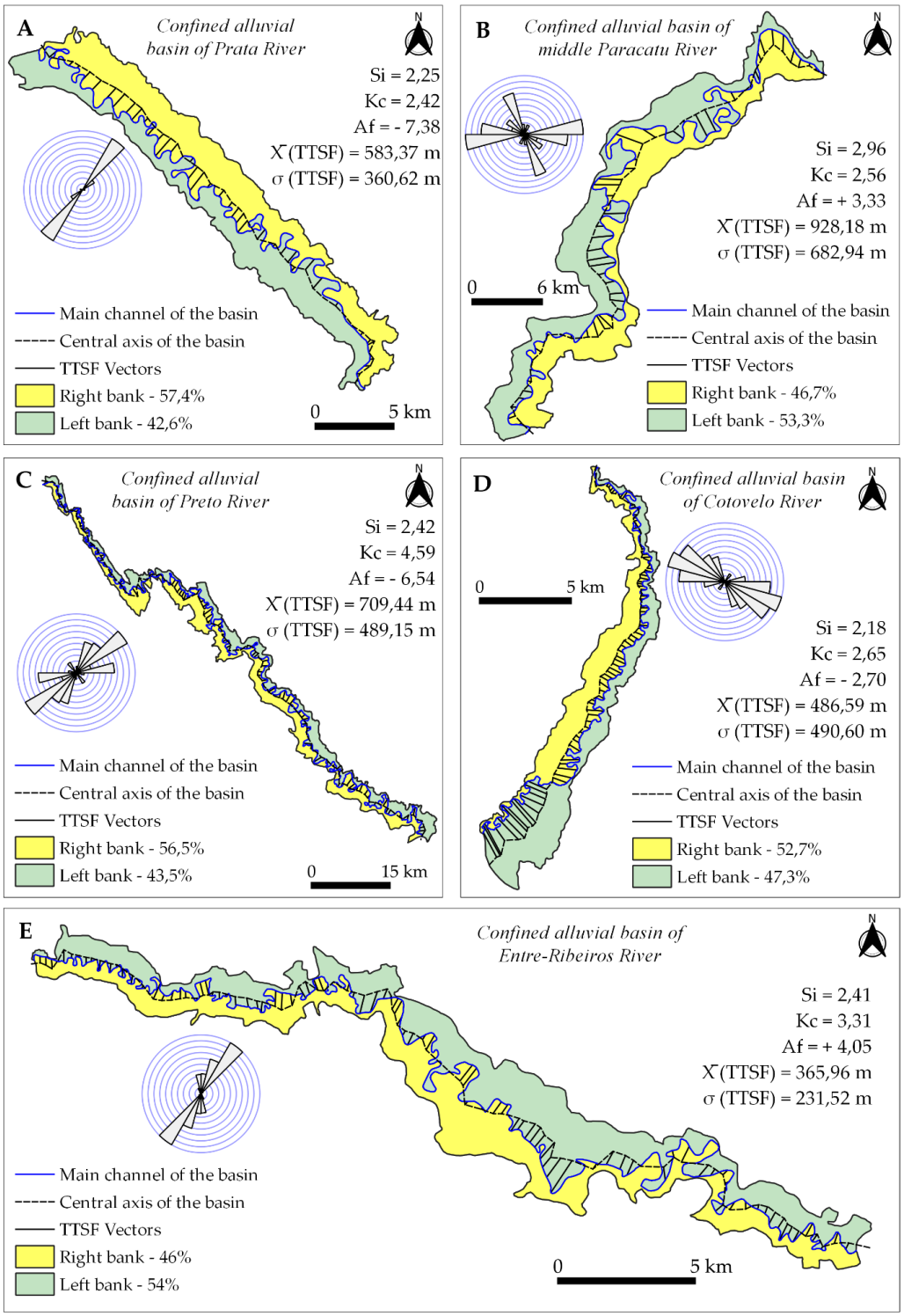

Figure 8. Confined alluvial basins and compressed meanders of the Paracatu River catchment. A) Prata River basin; B) middle Paracatu River basin; C) Preto River basin; D) Cotovelo River basin; E) Entre-Ribeiros River basin. The polar histograms show the predominant direction of channel migration, based on the vectors used in the TTSF calculation. X (TTSF): arithmetic mean of the length (in m) of the vectors used in the TTSF calculation; σ (TTSF): standard deviation of the length (in m) of the vectors used in the TTSF calculation.

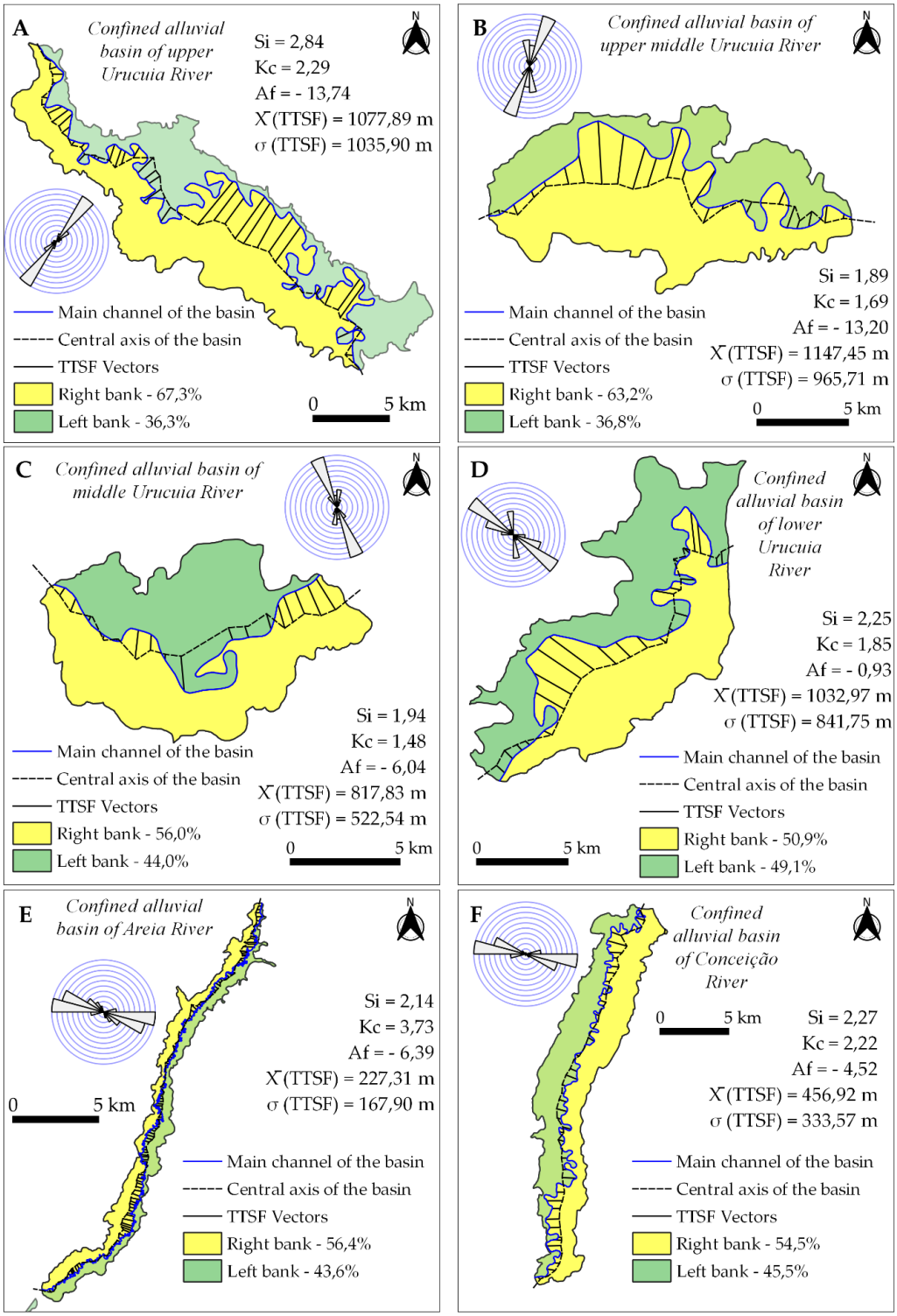

Figure 9. Confined alluvial basins and compressed meanders in the Urucuia River catchment. A) Upper Urucuia River basin; B) upper-middle Urucuia River basin; C) middle Urucuia River basin; D) lower Urucuia River basin; E) Areia River basin; F) Conceição River basin. The polar histograms show the predominant direction of channel migration, based on the vectors used in the TTSF calculation. X (TTSF): arithmetic mean of the length (in m) of the vectors used in the TTSF calculation; σ (TTSF): standard deviation of the length (in m) of the vectors used in the TTSF calculation.

Within the confined alluvial basins, compressed meander forms have emerged as distinctive components of the landscape (**Figure 10**). Compressed meanders are typical of sedimentary environments generated by reduced flow velocity in the fluvial channel, which may result from straightforward controls exerted by lithological resistance

or from tectonic processes such as upstream subsidence, downstream uplift, tilting, and doming (Howard, 1967; Holbrook; Schumm, 1999; Ramasamy et al., 2011). Such morphologies have been described in various settings, underscoring their applicability as diagnostic criteria for detecting recent tectonic movements (Ramasamy et al., 2011; Souza; Rossetti, 2011; Vargas et al., 2014; Alves; Rossetti, 2015; Sousa; Oliveira, 2016).

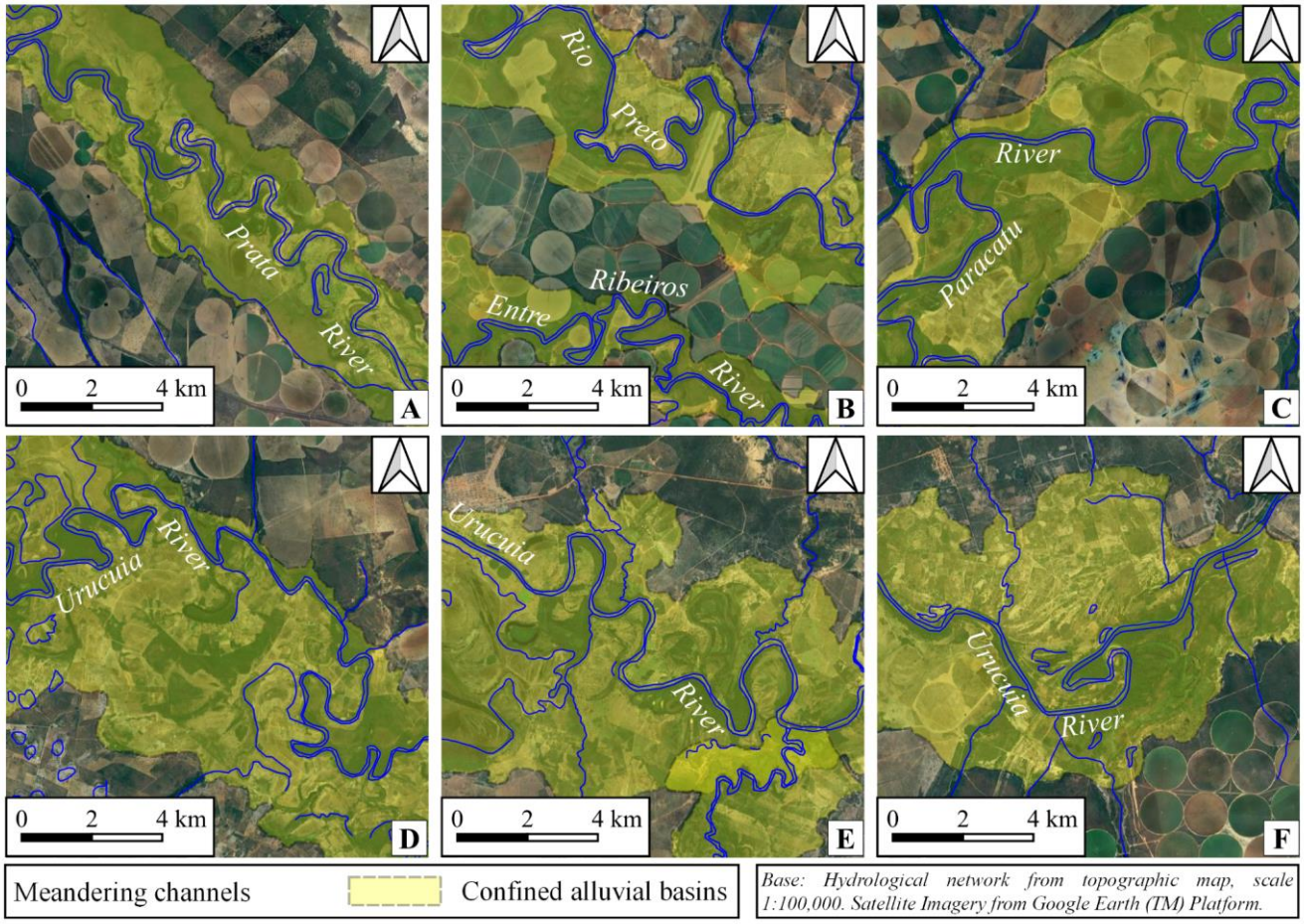

Figure 10. Sections of compressed meanders within confined alluvial basins. A) Prata River basin, near the confluence with the Paracatu River, under influence of the Galena-João Pinheiro fault system. B) Preto and Ribeirão Entre-Ribeiros Rivers, near craton–fold belt tectonic contact. C) Middle valley of the Paracatu River, within the Paracatu Depression. D) Upper Urucuia River valley, under influence of the São Domingos fault zone and interference of Meso-Cenozoic sills. E) Upper-middle valley of the Urucuia River, under influence of the São Domingos fault zone and interference of Meso-Cenozoic sills. F) Lower valley of the Urucuia River, under structural control by Meso-Cenozoic weakness zone.

4.1.1 Kc

Higher Kc values indicated more elongated and confined basins. The Entre-Ribeiros (Kc = 4.59), Areia (Kc = 3.73), and Preto River (Kc = 3.31) basins had the highest Kc values. The first two basins lie within the directional tectonic control zone with mapped fractures and faults tied to Brasiliano tectonics. Substrate resistance to fluvial incision, limiting valley widening, also enhanced their elongation.

A second-tier, lower Cotovelo River basin (Kc = 2.65), middle Paracatu River basin (Kc = 2.56), and Prata River basin (Kc = 2.42) share fluvial beds hosted by Upper Pleistocene–Holocene alluvium and are bounded by terrace escarps (Bragança, 2022).

Next are the upper Urucuia (Kc = 2.29) and the Conceição River (Kc = 2.22) basins, where the channel reaches are strongly structurally controlled by the São Domingos fault zone in the former and by the NNW-SSE shear zone in the latter. The lowest Kc values occurred in the lower, upper-middle Urucuia River basin (Kc = 1.69), and middle Urucuia River basin (Kc = 1.48), which were adjusted for structural control by the São Domingos fault but with

interference from Meso-Cenozoic structural trends in the form of imposed sills and lowered or tilted blocks, producing widened, rounded basins.

Overall, the confined basins in the Paracatu River catchment are more elongated than those in the Urucuia River catchment. This suggests greater directional control of the drainage network in Paracatu and, conversely, more frequent lithostructural controls oriented perpendicular to drainage in the Urucuia catchment, which is consistent with the pronounced meandering along the Urucuia River valley. Although subtle, differences in Kc reinforce the possibility of isolated block movements (Hare; Gardner, 1985), particularly for basins situated within or on the margin of the Paracatu Structural High.

4.1.2 Si

The highest Is values occurred in the Entre-Ribeiros (Si = 2.41), Preto (Si = 2.42), and upper Urucuia River (Si = 2.84) basins, and there was a close correlation between channel traces and mapped fractures/faults related to Brasiliano tectonics.

The second group, the Prata (Si = 2.25), Cotovelo (Si = 2.18), lower Urucuia (Si = 2.25), Areia (Si = 2.14), and Conceição River (Si = 2.27) basins, showed moderately high Si values. Except for the Prata River basin, which correlates with an extension of the Galena-João Pinheiro fault), these basins correlate with structural trends of the Meso-Cenozoic event and may be subject to imposed sills (uplifted blocks) or subsidence within fault zones (grabens, structural weakness). Si is comparatively lower in the upper-middle and middle Urucuia River basins (Si = 1.89 and 1.94, respectively), where meandering reflects adjustment to the São Domingos fault zone and interference from Meso-Cenozoic sills.

The lowest Si occurs in the middle Paracatu River basin, fully within the Paracatu Depression geomorphological region, where zones of structural weakness in the bedrock largely correlate with common karstic depressions (Almeida et al., 2011), where carbonate rocks predominate (Lagoa do Jacaré and Serra da Saudade Formations).

Si and Kc tended to be larger in the Paracatu catchment-confined basins than in those of the Urucuia catchment, reflecting the stronger structural confinement of a longer Urucuia trunk channel by the São Domingos fault. In Paracatu, Si and Kc variability indicates that most assessed basins lie on tributaries and are therefore subject to partially independent controls. In general, more elongated areas (higher Kc) confine more sinuous channels (higher Si), whereas more circular areas (lower Kc) host less sinuous channels (Si); the differences are modest, implying a broadly uniform response consistent with subsidence across all areas.

Even so, a degree of correlation between Si and Kc can be observed in the form and behaviour of confined alluvial basins. More elongated areas (higher Kc) tend to host more sinuous channels (higher Si). Conversely, more circular areas (lower Kc) confine the less sinuous channels (lower Si). The differences were modest; in practice, the Si and Kc values were close and fairly uniform, yielding a positive direct correlation for each confined alluvial basin assessed. This uniformity may be related to the subsidence behaviour common to all areas evaluated.

4.1.3 Basin Af

In the Paracatu River catchment, the confined basins were generally *symmetric* (Af < 5), as in the middle Paracatu (Af = 3.33), Cotovelo (Af = 2.70), and Entre-Ribeiros River (Af = 4.05) basins, or only slightly asymmetrical (5 < Af < 10), as in the Prata (Af = 7.38) and Preto River (Af = 6.54) basins.

Af yielded significantly variable outputs in the Urucuia River catchment area. The upper (Af = 13.74) and upper-middle Urucuia River (Af = 13.20) basins were *moderately asymmetric* (10 < Af < 15), and the middle Urucuia (Af = 6.04) and Areia River (Af = 6.39) basins were *gently asymmetrical* basins (5 < Af < 10). Finally, the lower Urucuia (Af = 0.93) and Conceição River (Af = 4.52) basins were *symmetric* (Af < 5).

The Af values appear to be random when the two basins are compared. In the Urucuia River catchment, the asymmetry values decrease from upstream to downstream owing to progressive dissection and consequent adjustment of the drainage to a structural zone of weakness. This assessment found no counterpart in the Paracatu River catchment because only a single confined alluvial basin was mapped along the trunk river of the basin.

The confined alluvial basins mapped in the Paracatu River catchment were markedly more elongated than those in the Urucuia River catchment. This suggests stronger directional control of the drainage network, complementing the previous analysis of feature elongation. However, in the Urucuia catchment, it indicates the

presence of lithostructural controls positioned perpendicular to the drainage, as exemplified by the pronounced meandering previously described along the Urucuia valley. Although subtle, these values reinforce the possibility of block tectonics involving isolated blocks (Hare and Gardner, 1985), particularly in alluvial basins situated within or along the margins of the Paracatu Structural High.

In the confined alluvial basins of the Paracatu River catchment, the Preto and Entre-Ribeiros Rivers have approximately parallel courses trending NNW–SSE. The Preto River displays negative asymmetry, migrating towards the left bank (NE), whereas the Entre-Ribeiros River shows positive asymmetry, migrating towards the right bank (SW). This opposition indicates the presence of a probable positive block near their watershed or, alternatively, a dissection guided by parallel structural weaknesses, similar to their channels.

The confined alluvial basin of the Prata River is similar to the previous cases but is controlled by an extension of the Galena Fault. It displays positive asymmetry, and its migration towards the right bank displaces the channel NE, which correlates positively with the mapped position of the fault.

The confined alluvial basin of the Cotovelo River shows negative asymmetry, indicating migration towards the left bank; however, given the directional control exerted by SW–NE lineaments in this catchment, the channel shifts SE. In the Cotovelo River, channel migration is controlled by the presence of grabens (Bragança, 2022). The confined alluvial basin of the middle Paracatu River lies within karst terrain with dolines, and its lateral migration towards the right bank appears to be a local phenomenon.

All confined alluvial basins in the Urucuia catchment exhibited negative asymmetry, indicating preferential migration towards the left bank. This pattern also appears to result from strong directional control of the Urucuia River by the São Domingos Fault. Accordingly, the asymmetry magnitudes were much greater in the upstream confined alluvial basins (upper Urucuia River, upper–middle Urucuia River, and middle Urucuia River), indicating strong migration towards the left bank (NE). Similarly, the lower Urucuia, Conceição, and Areia Rivers show negative asymmetry; however, these are approximately parallel channels oriented SW–NE and are influenced by sills or small subsiding blocks.

4.1.4 TTSF

Two mean value groups for the TTSF were distinguished. The first set pertains to the confined alluvial basins in the Urucuia River catchment (upper, upper-middle and middle Urucuia alluvial basins); their mean TTSF values range from -0,22 to - 0,28, implying moderate tilt of the bed substrate (Cox, 1994; Burbank and Anderson, 2001; Keller; Pinter, 2002; Salvany, 2004) towards the left bank (NE), which is consistent with adjustment to the São Domingos fault zone and possible block movement along the margins of the Paracatu Structural High. These negative TTSF values correlated with the negative Af values (**Figures 8** and **9**). The second set encompasses the remaining confined alluvial basins of the lower Urucuia River basin and its tributaries, the Areia and Conceição River basins, as well as all the Paracatu River catchment-confined alluvial basins, with modular values $|TTSF| < 0.13$, implying a low tilt. Similarly, in the Paracatu catchment, the confined alluvial basins showed (absolute) values of < 0.13. Therefore, they fall within settings subject to a low degree of bed substrate tilt (Cox, 1994; Burbank; Anderson, 2001; Keller; Pinter, 2002; Salvany, 2004).

However, in all cases, the standard deviation in both catchments lies between 0.34 and 0.53. This prevents complete dismissal of the substrate tilt and points to the movement of small blocks, whether due to accommodation and reactivation of ancient anisotropies or to the dynamics of the Paracatu Structural High.

A more detailed assessment of the TTFS values indicates that the channel behaviour is complex and distinctive within each confined alluvial basin, an interpretation reinforced by the Af values described previously. The confined alluvial basin of the Cotovelo River shows moderate to pronounced values over most of the channel, explaining its position along the left bank; near the Paracatu confluence; however, the channel abruptly migrates to the right bank ($0.7 < TTSF < 1.0$), a case explained by graben dynamics that accommodate this basin (Bragança, 2022). The second basin with the most expressive TTSF values is the middle Paracatu River basin, where the index indicates pronounced channel migration within the area, with meanders occupying much of its width ($-0.8 < TTSF < 0.8$). Within the confined alluvial basin of the Preto River, the channel tends to wander across the plain, alternately along the left and right banks, although a more perceptible positioning towards the NE (left bank) is evident, as indicated by Af. Although wandering, the channel in the confined alluvial basin of the Entre-Ribeiros River shows moderate migration within the basin, with several pronounced shifts towards the left bank (NE) that are more expressive than in the opposite direction; Af values are inconclusive here. Finally, the confined alluvial basin of

the Prata River exhibited the least channel wandering within the plain, indicating a low to moderate degree of substrate tilt despite a notable Af.

The TTSF values for the confined alluvial basins of the Urucuia catchment strongly corroborate the asymmetry analyses. The confined alluvial basin of the Upper Urucuia River shows moderate to pronounced TTSF values, indicating block tilting that justifies channel migration towards the left bank within the basin; values towards the opposite bank are only low to moderate. The same scenario is indicated by TTSF values for the confined alluvial basins of the upper–middle and middle Urucuia River basins (-1.0 < TTSF < -0.4). In contrast, the TTSF values for the confined alluvial basins of the middle and lower Urucuia River basins are lower than those upstream, which describes a reach of the Urucuia River oriented NW–SE that has begun to come under the influence of SW–NE structures and of the regional structural grain that controls the São Francisco River. Even so, a slight migration towards the left bank (NW) was observed, indicative of block tilting in that direction near the margin of the Paracatu Structural High, as suggested by the asymmetry values.

Finally, the assessment of the TTSF of the tributaries remained consistent with that of the catchment's trunk channel. The confined alluvial basin of the Conceição River accommodates a meandering channel with a strong tendency to shift towards the left bank (-0.8 < TTSF < -0.4). Finally, the confined alluvial basin of the Areia River accommodates a channel whose lateral migration is moderate along the length of its upper valley until, near the mouth, it undergoes a pronounced shift towards the left bank, under the influence of the same block that controls fluvial dynamics in the upper Urucuia River basin. This behaviour was corroborated by the asymmetry values.

Taken together, the TTSF values indicate only a slight bed tilt within the basins, whereas Af suggests only modest channel migration within the floodplains. High Af values indicated areas with the potential to tilt and influence drainage (Keller; Pinter, 2002). Therefore, multiple lines of evidence indicate possible block tilting in this area.

Conversely, the drainage system within these basins is out of equilibrium in relation to other sedimentation reaches and channels, supporting the hypothesis that the vertical movement of fault-bounded blocks may occur, which are interpreted as fragments of the Paracatu Structural High. The second possibility is the reactivation and accommodation of regional macrostructures associated with the craton and mobile belt, driven by the kinematics of the South American Plate. The movement of these isolated blocks may be inferred from the disposition of sedimentation basins along major Precambrian and Meso-Cenozoic fault zones as interrupted and isolated segments between straight reaches in the same fluvial channel. These straight reaches were invariably entrenched in the bedrock. The mutual arrangement of these confined alluvial basins, whether parallel or perpendicular, reinforces the interpretation of the lithostructural conditioning.

4.1.5 Principal directions from TTSF-vector histograms

In 10 of the confined alluvial basins, the histograms indicated that channel migration occurred perpendicular to the recognised structural direction for the area (from structural maps and mapped lineaments). This suggests that these structural directions imposed the recent conditioning of drainage, controlled subsiding blocks, and the imposition of sills.

The only exception is the middle Paracatu River basin along the trunk river, located upstream of the Serra da Maravilha within a doline sector (Almeida et al., 2011), which appears to combine karst control with the Precambrian weak lines of the Galena-João Pinheiro fault system.

The middle-lower Preto, lower Prata, and upper Urucuia River basins align with the reverse-fault trends of the Precambrian age. The middle Paracatu, Cotovelo, Conceição, and Areia River basins are adjusted to structural directions associated with the Meso-Cenozoic tectonic event; the first three basins evidence of subsidence. A similar subsidence-indicative morphology was observed in the middle and lower Urucuia River basins, although these last two align with a major SW-NE lineament that controls a ~180 km reach of the São Francisco River to the north-east of the study area.

4.2 Morphology of compressed-meander reaches

Within the confined alluvial basins, the channels displayed sinuous traces in the form of compressed meanders. Several factors explain this morphology, notably the subsident character of the basins and the inflow of

discharge and sediment load from tributaries entering them, such as the upper Urucuia , upper-middle Urucuia , middle Urucuia , Conceição , and Cotovelo River basins.

In the Conceição and Cotovelo river basins, sediment accumulation areas were elongated and bounded by steep, pronouncedly rectilinear terrace scarps (**Figure 11**), strongly supporting the hypothesis of subsiding blocks (Guedes et al., 2006; Bragança, 2022) and evidence of landscape dissection. Regionally, the Cotovelo River basin stands out as a barbed tributary, as a subsident feature, and as Holocene in age (Bragança, 2022). Remarkably, the Cotovelo floodplain receives at least four tributaries on its right bank (Bragança, 2022).

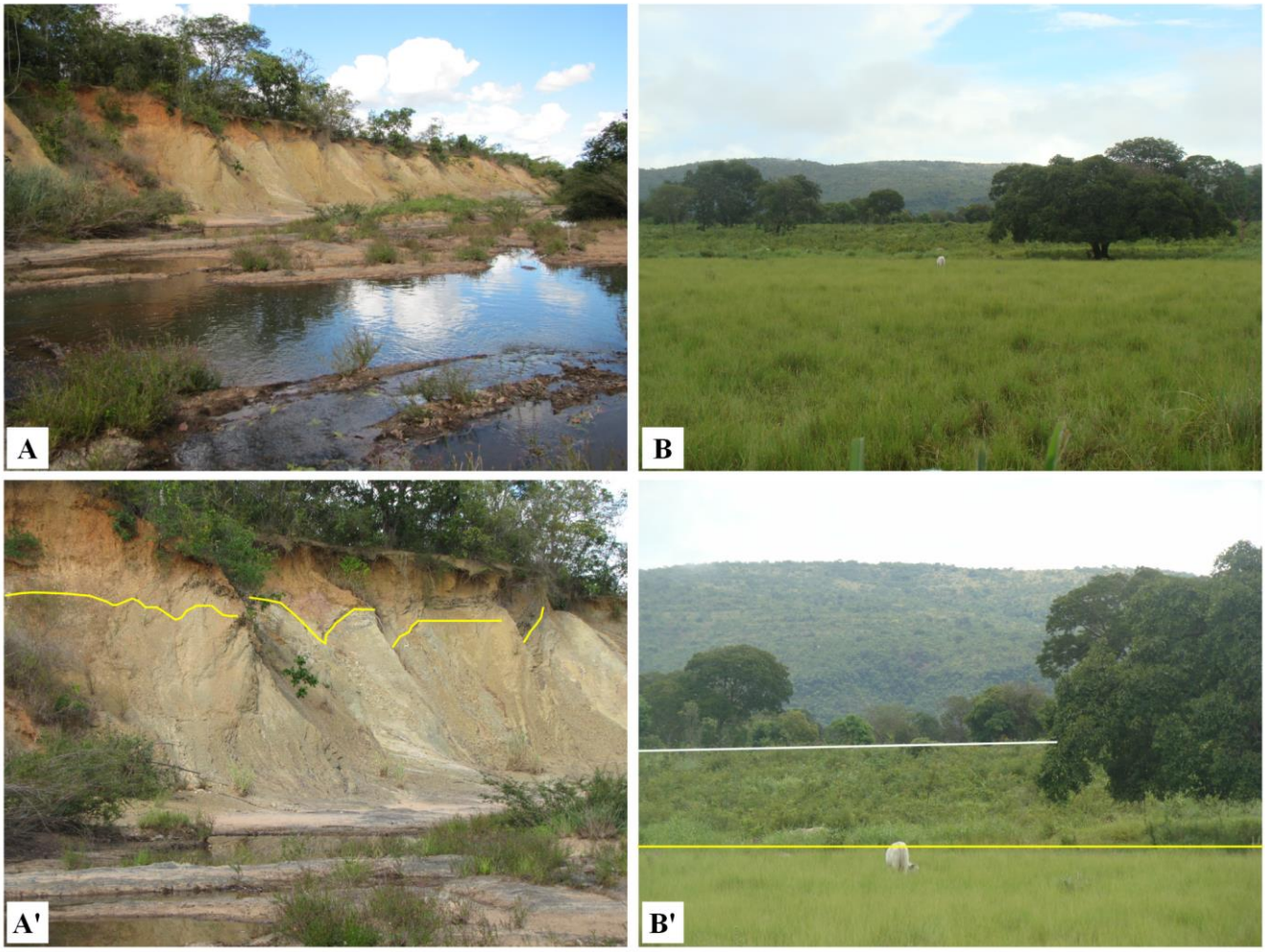

Figure 11. Terrace scarps in the Cotovelo River basin. A) Upstream sector of the fluviolacustrine plain, bounded by high terrace scarps resulting from the dissection of metapelites of the Serra da Saudade formation, into the NNW-SSE shear zone. A') Detail of photograph A: Base of Pleistocene terrace indicated by the yellow line and dated at this location at 28,550 (± 4,880) years. B) Panoramic view from within the Cotovelo River fluviolacustrine plain; Pleistocene terraces bound the plain. B') Detail of photograph B: Pleistocene terrace, dated at 12,180 (± 985) years; the yellow and white lines indicate the base and top of the scarp, respectively. Photographs taken near the CODEVASF Farm, in the municipality of Brasilândia de Minas. In the background, the Serra do Boqueirão Plateau. Photographs: collection of the first author.

The Prata River basin shows a similar morphology and interpretation (**Figure 12**), although there is no significant tributary inflow.

The lower Urucuia, Entre-Ribeiros, and middle Paracatu River basins show evidence of sill control. Within these areas, compressed meanders result from continual lateral migration under near-zero longitudinal gradients, which force the remobilisation of transported sediments and create obstacles to flow. The lower Urucuia River basin receives only first- and second-order tributaries, and its trunk channel wanders across the plains. The middle Paracatu River basin valley receives, upstream, the Prata River, which adds discharge and sediment load to the trunk river, and downstream, the inflow and sediment input of the Entre Ribeiros River, potentially producing the

highest calculated Si (2.96), owing to the added sediment load and its location within the eponymous depression, along with backwater effects from downstream inflow.

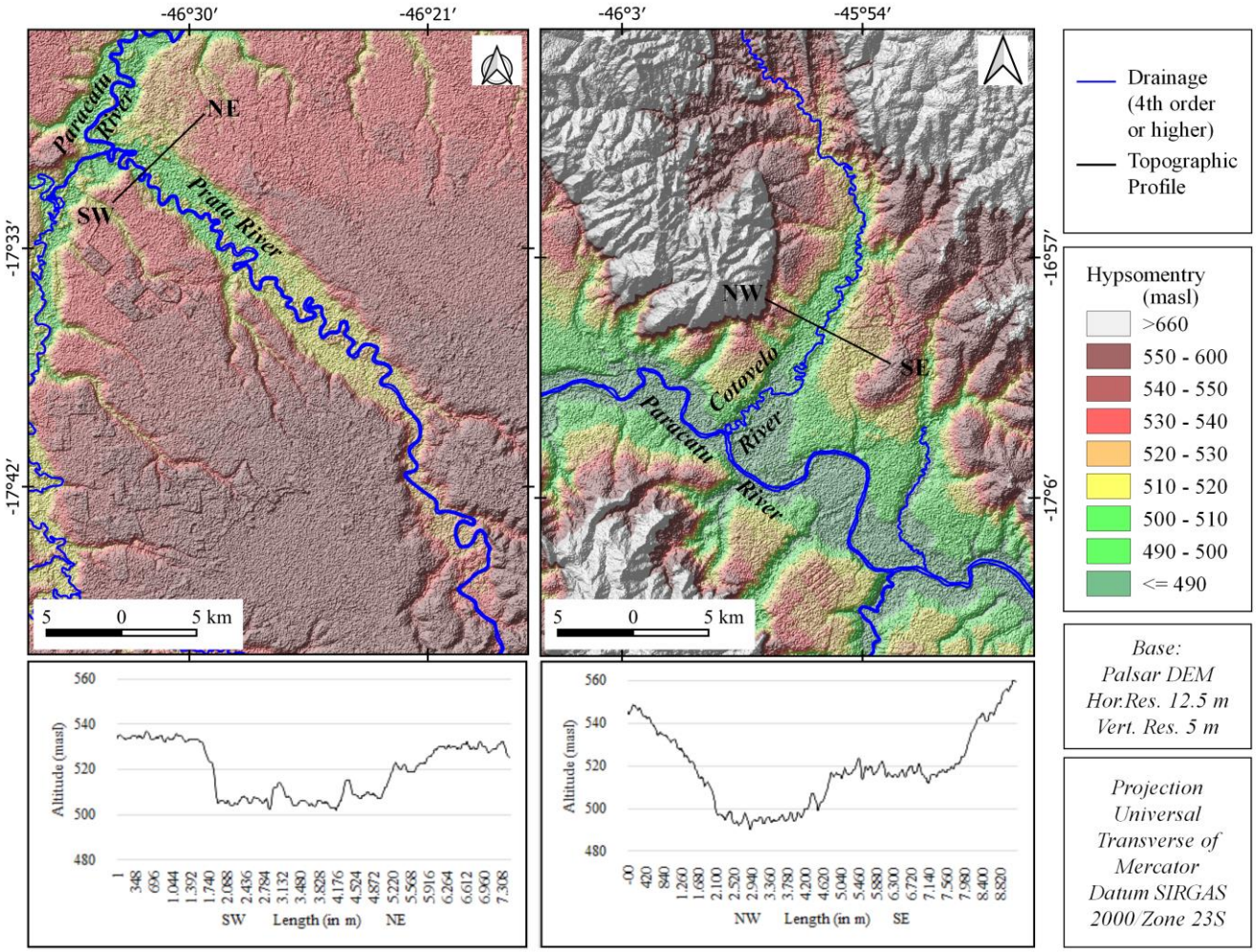

Figure 12. Morphology of the channels of the Prata and Cotovelo Rivers, showing the entrenchment of the lower valley and the alluvial basin confined by elevated edges. Note the sinuosity of channels, indicative of compressed meanders.

In the Conceição, Cotovelo, and Entre-Ribeiros River basins, the channel course and sedimentation are strongly structurally controlled; here, terrace scarps laterally confine the main channel dynamics.

Finally, the Preto, trending NNW-SSE, and Areia, trending NE-SW, River basins are also strongly lithostructurally controlled. Trunk channels are entrenched partly in the sediment and partly in the bedrock, with comparatively modest terrace packages and lower sinuosity. These basins display meandering patterns that record mixed morphogenesis, some of which reflect sedimentary dynamics controlled by pronounced bedrock sills, whereas others are direct consequences of channel entrenchment along lines of bedrock weakness.

5. Conclusions

In NW Minas Gerais State, within the contact zone between the São Francisco Craton and Brasília Fold Belt and within the deformed cratonic cover (foreland basin), drainage anomalies reveal a combination of geological, geomorphological, and structural factors at multiple scales. They also recorded the evolution of the regional relief and provided an explanatory framework for the drainage network. In this setting, confined alluvial basins are a common regional hydrogeomorphological feature.

The hydrogeomorphological and structural complexity of the territory indicates that the ongoing reactivation of the Paracatu Structural High and the São Francisco Craton–Brasília Fold Belt contact zone has made these important features on the arrangement of the regional drainage network.

Morphodynamics within confined alluvial basins are strongly influenced by structural and tectonic factors. Hydrogeomorphological processes are also important. Within these basins, overbank flooding is common, whereas outside those channels, they tend to remain confined to their banks. This process is expressed geomorphically by higher soil moisture within confined alluvial basins, even during the dry season, relative to other sectors of the landscape, including terraces. The regional climatic seasonality corroborates the geomorphological characteristics of confined alluvial basins and aligns with the concepts of depressed wetlands and floodplains.

These small geomorphic features, which reveal clear structural control, allow for the inference of the reactivation of zones of weakness and the nucleation of new, small normal faults during the Plio-Pleistocene. Specifically, confined alluvial basins and the alteration of primary and secondary rock structures by fractures oriented in two principal directions (NNW-SSE and SW-NE) have a direct relationship. Simultaneously, hydrogeomorphological processes are more active within basins locally, continuously, and persistently.

Confined alluvial basins are regional features with a subsident character and embody a pattern arising from the dynamics of small blocks resulting from the fragmentation of the Paracatu Structural High and reactivation of the craton–fold belt contact. Because channels are moderately asymmetric within these areas and pronounced asymmetries are also present, sedimentary dynamics appear to be controlled by block tectonics with discrete, differentiated vertical movements. In all the confined alluvial basins, observable drainage features reflected active ongoing fluvial morphodynamics.

Author's contributions: Conception, M.T.R.B. and L.F.P.B.; methodology, M.T.R.B.; software, M.T.R.B.; validation, M.T.R.B.; L.F.P.B. and D.O.; formal analysis, M.T.R.B.; research, M.T.R.B.; resources, M.T.R.B. and L.F.P.B.; data preparation, M.T.R.B.; article writing, M.T.R.B.; revision, M.T.R.B. and L.F.P.B.; supervision, L.F.P.B. and D.O.; acquisition of funding, L.F.P.B. All authors have read and agreed with the published version of the manuscript.

Funding: This research was partially funded by the Fundação de Amparo à Pesquisa do Estado de Minas Gerais (FAPEMIG; grant number APQ-00770-24).

Acknowledgments: We would like to thank the members of the RIVUS (Geomorphology and Water Resources Research Group - https://rivusufmg.wixsite.com/home) for their contributions and the editor and referees for their insightful comments and suggestions.

Conflict of Interest: The authors declare no conflicts of interest.

References

1. ALKMIM, F.F.; BRITO-NEVES, B.B.; ALVES J.A.C. Arcabouço tectônico do Cráton do São Francisco - Uma revisão. In: DOMINGUEZ; J.M.L.; MISI, A. (eds.) **O Cráton do São Francisco**. SBG/Núcleo BA/SE, 1993. pp. 45-62.
2. ALKMIM, F.F.; MARTINS-NETO, M.A. A Bacia Intracratônica do São Francisco: Arcabouço estrutural e cenários evolutivos. In PINTO, C.P.; MARTINS-NETO, M.A. (eds.). **Bacia do São Francisco: Geologia e Recursos Naturais**. Belo Horizonte, SBG/Núcleo Minas Gerais, 2001. p. 9-30.
3. ALMEIDA, A.C.S.; VARAJÃO, A.F.D.C.; VARAJÃO, C.A.C.; GOMES, N.S.; VOLMER-RIBEIRO, C. Domínios geomorfológicos na área de ocorrência dos depósitos de espongilito da região de João Pinheiro, Minas Gerais, Brasil. **Revista da Escola de Minas**, v. 64, n. 3, p. 299-304, 2011.
4. ALVES, F.C.; ROSSETTI, D.F. Análise morfoestrutural e neotectônica na porção norte da Bacia Paraíba (PB). **Revista Brasileira de Geomorfologia**, v. 16, n. 4, p. 559-578, 2015.
5. ASF-DAAC. ALOS PALSAR Radiometric Terrain Corrected high resolution 2015; Includes Material © JAXA/METI 2007. Accessed through ASF-DAAC 27 may 2018. DOI: https://doi.org/10.5067/JBYK3J6HFSVF.
6. BARCELOS, J.H.; SUGUIO, K. Ambiente de sedimentação da Formação Areado, Cretáceo Inferior da Bacia Sanfranciscana, MG. **Revista Brasileira de Geociências**, v. 10, p. 237 – 242, 1980.
7. BISHOP, P. Drainage rearrangement by river capture, beheading and diversion. **Progress in Physical Geography**, v. 19, n. 4, p. 449-473, 1995.
8. BRAGANÇA, M.T.R. **Morfoestrutura e Morfotectônica no Noroeste de Minas Gerais: o graben holocênico do baixo Ribeirão Cotovelo e seu enquadramento na hidrogeomorfologia regional**. Tese (Doutorado em Geografia Física) - Faculdade de Filosofia, Letras e Ciências Humanas, Universidade de São Paulo, São Paulo, 2022a. https://doi.org/10.11606/T.8.2022.tde-19072022-184004
9. BRAGANÇA, M.T.R.; BARROS, L.F.P.; OLIVEIRA. D. Curvaturas anômalas e segmentos retilíneos de canais como evidência de controle lito-estrutural da rede de drenagem no noroeste de Minas Gerais. In: SIMPÓSIO BRASILEIRO DE GEOGRAFIA FÍSICA APLICADA, 19. 2022, Rio de Janeiro. Antropoceno: das transformações às metamorfoses das paisagens e do mundo. **Anais…** Rio de Janeiro: IGEOG/PPGEO/UERJ, 2022a. p. 13-17.

10. BRAGANÇA, M.T.R.; BARROS, L.F.P.; OLIVEIRA, D. Dissecação fluvial pleistocênica e holocênica na margem esquerda do Rio São Francisco, em Minas Gerais. In: SIMPÓSIO BRASILEIRO DE GEOGRAFIA FÍSICA APLICADA, 19, 2022, Rio de Janeiro. Antropoceno: das transformações às metamorfoses das paisagens e do mundo. **Anais…** Rio de Janeiro: IGEOG/PPGEO/UERJ, 2022b. v. 1. p. 18-22.
11. BRAGANÇA, M. T. R.; BARROS, L. F. P.; OLIVEIRA, D. Morphotectonic and morphostructural investigation in northwestern Minas Gerais State, Brazil: a lineament mapping assessment. **Revista Brasileira de Geomorfologia,** v. 24, p. e2322, 2023a. DOI: https://doi.org/10.20502/rbg.v24i2.2322
12. BURBANK, D.W.; ANDERSON, R.S. **Tectonic Geomorphology**. Oxford: Blackwell Science. 2001.
13. BURNETT, A.W.; SCHUMM, S.A. Alluvial-river response to neotectonic deformation in Louisiana and Mississipi. **Science**, v. 222, p. 49-50, 1983.
14. CAMPOS, J.E.G.; DARDENNE, M.A. A glaciação neopaleozoica na porção meridional da Bacia Sanfranciscana. **Revista Brasileira de Geociências,** v. 24, n. 2, p. 65-76, 1994.
15. CAMPOS, J.E.G.; DARDENNE, M.A. Origem e evolução tectônica da Bacia Sanfranciscana. **Revista Brasileira de Geociências**, v. 27, n. 3, p. 283-294, 1997a.
16. CAMPOS, J.E.G.; DARDENNE, M.A. Estratigrafia e sedimentação da Bacia Sanfranciscana: uma revisão. **Revista Brasileira de Geociências**, v. 27, n. 3, p. 269-282, 1997b.
17. CHUVIECO, E. **Fundamentos de teledetección espacial**. Madrid: Rialp, 1996.
18. COTTON, C.A. Fault valleys and shutter ridges at Wellington. **New Zealander Geographer**, v. 7, p. 62-68, 1951.
19. COX, R. T. Analysis of drainage-basin symmetry as a rapid technique to identify areas of possible quaternary tilt block tectonics: as example from the Mississipi Embayment. **Geological Society of América Bulletin**, v. 106, p. 571-581, 1994.
20. CPRM; COMIG. **Folha SE.23-V-D - João Pinheiro.** Programa Levantamentos Geológicos Básicos do Brasil Carta Geológica - Escala 1:250.000. Belo Horizonte: CPRM; COMIG, 2003a. Scale 1:250,000.
21. CPRM; COMIG. **Folha SE.23-V-B - São Romão.** Programa Levantamentos Geológicos Básicos do Brasil Carta Geológica - Escala 1:250.000. Belo Horizonte: CPRM; COMIG, 2003b. Scale 1:250,000
22. DEFFONTAINES, B.; CHOROWICZ, J. Principles of drainage basin analysis from multisource data: Application to the structural analysis of the Zaire Basin. **Tectonophysics**, v. 194, p. 237-263, 1991.
23. DRACHAL, J.; DEBOWSKA, A. Towards a More Realistic Depiction of the Earth's Surface on Maps. **Pure and Applied Geophysics**, v. 171, p. 1061-1075, 2014. DOI 10.1007/s00024-013-0684-8.
24. DUVALL, A.R.; HARBERT, S.A.; UPTON, P.; TUCKER, G.E.; FLOWERS, R.M.; COLLETT, C. River patterns reveal two stages of landscape evolution at an oblique convergent margin, Marlborough Fault System, New Zealand, **Earth Surf. Dynam.**, 8, 177–194, https://doi.org/10.5194/esurf-8-177-2020, 2020.
25. FIRMINO, I.G.; SOUZA FILHO, E.E. Análise de Padrões e de Anomalias de Drenagem da Porção Média da Bacia do Rio Tibagi (PR). **Revista Brasileira de Geomorfologia (Online)**, São Paulo, v.18, n.1, p.37-49, 2017.
26. FRAGOSO, D.G.C.; UHLEIN, A.; SANGLARD, J.C.D.; SUCKAU, G.L.; GUERZONI, H.T.G.; FARIA, P.H. Geologia dos Grupos Bambuí, Areado e Mata da Corda na Folha Presidente Olegário (1:100.000), MG: Registro deposicional do Neoproterozóico ao Neocretáceo da Bacia do São Francisco. **Geonomos**, v. 19, p. 28-38, 2011. http://dx.doi.org/10.18285/geonomos.v19i1.60.
27. GOMES, C.S.; MAGALHÃES JR, A.P. Classes hidrogeomorfológicas de áreas úmidas em Minas Gerais. **Revista Brasileira de Geomorfologia (Online)**, v.21, n.2, (Abr-Jun) p.313-327, 2020. http://dx.doi.org/10.20502/rbg.v21i2.1794
28. GUEDES, I.C.; SANTONI, G.C.; ETCHEBEHERE, M.L.C.; STEVAUX, J.C.; MORALES, N.; SAAD, A.R. Análise de perfis longitudinais de drenagens da bacia do Rio Santo Anastácio (SP) para detecção de possíveis deformações neotectônicas. **Rev UnG Geociências**, v. 5, p. 75–102, 2006.
29. GUERASIMOV, I.P.; MESCHERIKOV, J.A. Morphostructure. In: **Geomorphology, Encyclopedia of Earth Science**. Springer, Berlin, Heidelberg, 1968. p. 731-732.
30. HARE, P.W.; GARDNER, T.W. Geomorphic indicators of vertical neotectonism along converging plate margins, Nicoya Peninsula, Costa Rica. In MORISAWA, M.; HACK, J.T. (Eds.) **Tectonic Geomorphology**. Allen and Unwin, Boston, 1985. p. 75–104.
31. HASUI, Y. Neotectônica e aspectos fundamentais da tectônica ressurgente no Brasil. I Workshop sobre Neotectônica e Sedimentação Cenozoica Continental no Sudeste Brasileiro. 1., 1990. Belo Horizonte. **Anais**... Belo Horizonte: SBG-Núcleo Minas Gerais. 1990. p. 1–31.
32. HASUI, Y.; HARALYI, N.L.E. Aspectos lito-estruturais e geofísicos do soerguimento do Alto Paranaíba. **Geociências**, v. 10, p. 57-77, 1991.
33. HOLBROOK, J., SCHUMM, S.A. Geomorphic and sedimentary response of rivers to tectonic deformation: a brief review and critique of a tool for recognizing subtle epeirogenic deformation in modern and ancient settings. **Tectonophysics,** Amsterdam, v. 305, p. 287–306. 1999.

34. HOWARD, A. D. Drainage analysis in geologic interpretation: A summation. **The American Association of Petroleum Geologists Bulletin**, v. 51, p. 2246-2259, 1967.
35. IBGE. **Geomorfologia**. Base de Dados Espacial 1:250.000, Brasil. Versão_2023. Disponível em: https://www.ibge.gov.br/geociencias/informacoes-ambientais/geomorfologia/10870-geomorfologia.html Acesso em 9 jul 2025.
36. NUNES, B.A.; RIBEIRO, M.I.C.; ALMEIDA, V.J.; NATALI FILHO, T. (Coords.). **Manual Técnico de Geomorfologia**. Rio de Janeiro: Fundação IBGE, 1995.
37. KATTAH, S.S. **Análise faciológica e estratigráfica do Jurássico Superior/Cretáceo Inferior na porção meridional da Bacia Sanfranciscana, oeste do Estado de Minas Gerais**. Dissertação (Mestrado em Geologia). Escola de Minas, Universidade Federal de Ouro Preto, Ouro Preto, 1991. 227p.
38. KELLER, E.A.; PINTER, N. A**ctive Tectonics: Earthquakes, Uplift and Landscape.** New Jersey: Prentice Hall, 2002.
39. LIMA, A.G. Rios de leito rochoso: aspectos geomorfológicos fundamentais. **Ambiência**, v.6 n.2 p. 339-354. 2010.
40. LOPES, E.E. **Proposta metodológica para validação de imagens de alta resolução do *Google Earth* para a produção de mapas**. Dissertação (Mestrado em Engenharia Civil). Centro Tecnológico da UFSC, Universidade Federal de Santa Catarina, Florianópolis, 2009. 112p.
41. LP-DAAC. Shuttle Radar Topography Mission (SRTM) 1 Arc-Second Global from 2018 was retrieved on 2018 06 08 from https://lta.cr.usgs.gov/SRTM1Arc, maintained by the NASA EOSDIS Land Processes Distributed Active Archive Center (LP DAAC) at the USGS Earth Resources Observation and Science (EROS) Center, Sioux Falls, South Dakota. 2018.
42. MANJORO, M. Structural control of fluvial drainage in the western domain of the Cape Fold Belt, South Africa. **Journal of African Earth Sciences**, Amsterdam, v. 101, p. 350–359. 2015.
43. MARPLE, R.T.; TALWANI, P. Evidence of possible tectonic upwarping along the South Carolina Coastal plain from an examination of river morphology and elevation data. **Geology**, Boulder, v. 21, p. 651-654, 1993.
44. MINAS GERAIS (Estado). Fundação Centro Tecnológico de Minas Gerais. **II Plano de Desenvolvimento Regional do Noroeste - Planoroeste**. Belo Horizonte, Fundação Centro Tecnológico de Minas Gerais. 1981.
45. MINAS GERAIS (Estado). Fundação Centro Tecnológico de Minas Gerais. **Diagnóstico Ambiental de Minas Gerais**. Belo Horizonte, Fundação Centro Tecnológico de Minas Gerais. 1983. 158p.
46. MOREIRA, A.A.N.; CAMELIER, C. Relevo. In: GALVÃO, M. G. (Ed.). **Geografia do Brasil, Região Sudeste**. Rio de Janeiro: Fundação Instituto Brasileiro de Geografia e Estatística, 1977. p. 1–50.
47. PANDEY, S. **Principles and applications of photogeology**. Nova Delhi: New Age International Publishers, 2001.
48. PARVIS, M. Drainage pattern significance in airphoto identification of soils and bedrocks. **Photogrammetric Engineering**, v. 16, p. 375-409, 1950.
49. PÉREZ-PEÑA, J.; AZAÑÓN, J.; BOOTH-REA, G.; AZOR, A.; DELGADO, J. Differentiating geology and tectonics using a spatial autocorrelation technique for the hypsometric integral. **Journal of Geophysical Research: Earth Surface,** v. 114, n. F2, F02018, 2009.
50. PERUCCA, L.P., ROTHIS, M.; VARGAS, H.N. Morphotectonic and Neotectonic Control on River Pattern in the Sierra de La Cantera Piedmont, Central Precordillera, Province of San Juan, Argentina. **Geomorphology**, v. 204, p. 673–82, 2014. https://linkinghub.elsevier.com/retrieve/pii/S0169555X13004728
51. QGIS Development Team. QGIS Geographic Information System (versão 3.22). 2023. Disponível em: <http://qgis.osgeo.org>.
52. PRODEMGE. Companhia de Tecnologia da Informação do Estado de Minas Gerais – Prodemge. Infraestrutura de Dados Espaciais, s/d. Disponível em: http://www.geo.prodemge.gov.br. Acesso em abr./2024.
53. RAMASAMY, S.M., KUMANAN, C.J., SELVAKUMAR, R., SARAVANAVEL, J. Remote sensing revealed drainage anomalies and related tectonics of South India. **Tectonophysics** 501, 41–51. 2011
54. REIS, H.L.S., ALKMIM, F.F., SILVA, L.C. O Cinturão neoproterozoico de antepaís da Faixa Brasília, Bacia do São Francisco (Brasil), características e principais traços tectônicos. In: Congresso Brasileiro de Geologia, 46. **Anais…** Sociedade Brasileira de Geologia (SBG), Santos. 2012.
55. REIS, H.L.S.; ALKMIM, F.F. Anatomy of a basin-controlled foreland fold-thrust belt curve: The Três Marias salient, São Francisco basin, Brazil. **Marine and Petroleum Geology**, v. 66, p. 711-731, 2015. https://doi.org/10.1016/j.marpetgeo.2015.07.013
56. REIS, H.L.S.; ALKMIM, F.F.; FONSECA, R.C.S.; NASCIMENTO, T.C.; SUSS, J.F.; PREVATTI, L.D. The São Francisco Basin. In: HEILBRON, M.; CORDANI, U.G.; ALKMIM, F.F. **São Francisco Craton, Eastern Brazil: tectonic genealogy of a miniature continent**. Switzerland: Springer, 2017. p. 117–43. https://doi.org/10.1007/978-3-319-01715-0_7.
57. RHEA, S. Evidence of uplift near Charleston, South Carolina. **Geology**, Boulder, v. 17, p. 311–315, 1989.
58. SAADI, A. **Ensaio sobre a morfotectônica de Minas Gerais: tensões intraplaca, descontinuidades crustais e morfogênese**. Tese (Professor Titular) – Instituto de Geociências, Universidade Federal de Minas Gerais, Belo Horizonte. 1991. 285p

59. SALAMUNI, E.; EBERT, H. D; HASUI, Y. Morfotectônica da Bacia Sedimentar de Curitiba. **Revista Brasileira de Geociências**, v. 34, n. 4, p. 469-478, 2004.
60. SALVANY, J.M. Tilting neotectonics of the Guadiamar drainage basin, SW Spain. **Earth Surface Processes and Landforms**, v. 29, n. 2, p. 145-160, 2004.
61. SCHOBBENHAUS, C.; CAMPOS, D.A; DERZE, G.R.; ASMUS, H.E. (Coords.). **Geologia do Brasil: texto explicativo do mapa geológico do Brasil e da área oceânica adjacente incluindo depósitos minerais**. Brasília: Departamento Nacional de Produção Mineral, 1984. 501 p.
62. SCHOBBENHAUS, C.; CAMPOS, D.A; DERZE, G.R.; ASMUS, H.E. **Mapa geológico do Brasil e da área oceânica adjacente incluindo depósitos minerais**. 2.ed. Ministério de Minas e Energia. CPRM – Serviço Geológico do Brasil, 1985. Scale 1:2.500.000.
63. SGARBI, G.N.C. The Cretaceous Sanfranciscan Basin, Eastern Plateau of Brazil. **Revista Brasileira de Geociências**, v. 30, n. 3, p. 450-452, 2000.
64. SORDI, M.V.; SALGADO, A.A.R.; CORDEIRO, C.M.; GOMES, A.A.T.; BARROS, L.F.P.; MAGALHÃES JR., A.P. Drainage network evolution and divide retreat along a passive margin: the permanence of disequilibrium under unfavorable natural conditions in eastern South America. **Physical Geography**, v. 43, p. 1-28, 2022. DOI: 10.1080/02723646.2022.2080798.
65. SOUGNEZ, N.; VANACKER, V. The topographic signature of Quaternary tectonic uplift in the Ardennes massif (Western Europe). **Hydrology and Earth System Sciences**, v. 15, p. 1095–1107, 2011
66. SOUSA, M.M.; OLIVEIRA, W. Identificação de feições anômalas dos sistemas de drenagem na região do Alto Juruá – AC/AM, utilizando dados de sensoriamento remoto. **Revista Brasileira de Geografia Física**, v. 9, n. 4, p. 1254-1267, 2016.
67. SOUZA, L.S.B.; ROSSETTI, D.F. Caracterização da rede de drenagem na porção leste da Ilha do Marajó e implicações tectônicas. **Revista Brasileira de Geomorfologia**, v. 12, n. 1, p. 69-83, 2011.
68. STRAHLER, A. N. Quantitative analysis of watershed geomorphology. **Transactions of the American Geophysical Union**, v. 8, n. 6, p. 913-920, 1957.
69. TWIDALE, C.R. River patterns and their meaning. **Earth-Science Reviews**, v. 67, p. 159–218, 2004.
70. VARGAS, K.B.; SORDI, M.V.; FORTES, E.; JAYME, N.S.; ALVES JR, A.P. Análise de anomalias de drenagem na área abrangida pela carta topográfica de Mauá da Serra – PR. **Revista Geonorte**, Edição Especial 4, v. 10, n.6, p. 23-28, 2014.
71. VILLELA, S. M.; MATTOS, A. **Hidrologia aplicada**. São Paulo: McGraw-Hill do Brasil, 1975. 245p.
72. VOLKOV, N.G.; SOKOLOVSKY, I.L.; SUBBOTIN, A.I. Effect of recent crustal movements on the shape of longitudinal profiles and water levels of rivers. In: INTERNATIONAL SYMPOSIUM ON RIVER MECHANICS. Bern: International Union of Geodesy and Geophysics, **Proceedings…** Bern, 1967.
73. ZERNITZ, E.R. Drainage patterns and their significance. **Journal of Geology**, 40, p. 498-521. 1932. http://dx.doi.org/10.1086/623976